Development of theoretical model correlating elastic modulus and porosity of bone

王, 心
九州大学大学院総合理工学府総合理工学専攻機械・システム理工学メジャー

2022

Thesis for the degree of Master

DEVELOPMENT OF THEORETICAL MODEL CORRELATING ELASTIC MODULUS AND POROSITY OF BONE

Interdisciplinary Graduate School of Engineering Science

Kyushu University

Mechanical and Systems Engineering

Bioenergy Engineering Laboratory

Wang Xin

Supervisor Mitsugu TODO

Submission Date: February 6th,2023

Abstract

The principal objectives of this study were to calculate the relationship between bone mineral density (porosity) and the Young's modulus of bone theoretically and compare with Keyak's results. In this study, bone is first considered as an ideal poroelastic medium. Through Cowin's research, the Young's modulus equation of cortical bone and cancellous bone (trabecular bone) was deduced under ideal conditions.

Afterwards, a micromechanical model for the Young's modulus of bone proposed by Wanger was introduced. The model incorporates the platelet-like geometry of the basic reinforcing unit, the presence of alternating thin and thick lamellae, and the orientations of the crystal platelets in the lamellae. The thin and thick lamellae are modeled as orthotropic composite layers made up of thin rectangular apatite platelets within a collagen matrix, and classical orthotropic elasticity theory is used to calculate the Young's modulus of the lamellae. Bone is viewed as an assembly of such orthotropic lamellae bent into cylindrical structures, and having a constant, alternating angle between successive lamellae. The micromechanical model employs a modified rule-of-mixtures to account for the two types of lamellae.

By introducing this model, the parameter Es(the highest elastic modulus of bone) in the macroscopic model was corrected using a variety of different theoretical equations to estimate the Young's modulus of normal bone, bone with osteopenia and bone with osteoporotic, and compared with Keyak's experimental data. In the study, through theoretical calculations, it is proved that the calculation results of the theoretical model are basically consistent with Keyak's experimental results, and it is found that the results obtained by using the HT model in the research are closer to Keyak's experimental results than the PB model.

Table of Content

1 Introduction

1.1 The structure of bone

A bone is a rigid organ that constitutes part of the skeleton in most vertebrate animals. Bones protect the various other organs of the body, produce red and white blood cells, store minerals, provide structure and support for the body, and enable mobility. Bones come in a variety of shapes and sizes and have complex internal and external structures. They are lightweight yet strong and hard and serve multiple functions.[1][2]

Bone is not uniformly solid, but consists of a flexible matrix (about 30%) and bound minerals (about 70%) which are intricately woven and endlessly remodeled by a group of specialized bone cells. Their unique composition and design allows bones to be relatively hard and strong, while remaining lightweight.

Bone matrix is 90 to 95% composed of elastic collagen fibers, also known as ossein, and the remainder is ground substance. The elasticity of collagen improves fracture resistance. The matrix is hardened by the binding of inorganic mineral salt, calcium phosphate, in a chemical arrangement known as bone mineral, a form of calcium hydroxyapatite. It is the mineralization that gives bones rigidity.

Bone is actively constructed and remodeled throughout life by special bone cells known as osteoblasts and osteoclasts. Within any single bone, the tissue is woven into two main patterns, known as cortical and cancellous bone, each with a different

appearance and characteristics.

The hard outer layer of bones is composed of cortical bone, which is also called compact bone as it is much denser than cancellous bone. It forms the hard exterior (cortex) of bones. The cortical bone gives bone its smooth, white, and solid appearance, and accounts for 80% of the total bone mass of an adult human skeleton. It facilitates bone's main functions—to support the whole body, to protect organs, to provide levers for movement, and to store and release chemical elements, mainly calcium. It consists of multiple microscopic columns; each called an osteon or Haversian system. Each column is multiple layers of osteoblasts and osteocytes around a central canal called the haversian canal. Volkmann's canals at right angles connect the osteons together. The columns are metabolically active, and as bone is reabsorbed and created the nature and location of the cells within the osteon will change. Cortical bone is covered by a periosteum on its outer surface, and an endosteum on its inner surface. The endosteum is the boundary between the cortical bone and the cancellous bone. The primary anatomical and functional unit of cortical bone is the osteon.[3]

Cancellous bone, also called trabecular or spongy bone, is the internal tissue of the skeletal bone and is an open cell porous network that follows the material properties of biofoams. Cancellous bone has a higher surface-area-to-volume ratio than cortical bone and it is less dense. This makes it weaker and more flexible. The greater surface area also makes it suitable for metabolic activities such as the exchange of calcium ions.

Cancellous bone is typically found at the ends of long bones, near joints, and in the interior of vertebrae. Cancellous bone is highly vascular and often contains red bone marrow where hematopoiesis, the production of blood cells, occurs. The primary anatomical and functional unit of cancellous bone is the trabecula. The trabeculae are aligned towards the mechanical load distribution that a bone experiences within long bones such as the femur. As far as short bones are concerned, trabecular alignment has been studied in the vertebral pedicle. Thin formations of osteoblasts covered in endosteum create an irregular network of spaces, known as trabeculae. Within these spaces are bone marrow and hematopoietic stem cells that give rise to platelets, red blood cells and white blood cells.

Trabecular marrow is composed of a network of rod- and plate-like elements that make the overall organ lighter and allow room for blood vessels and marrow. Trabecular bone accounts for the remaining 20% of total bone mass but has nearly ten times the surface area of compact bone.[4][5]

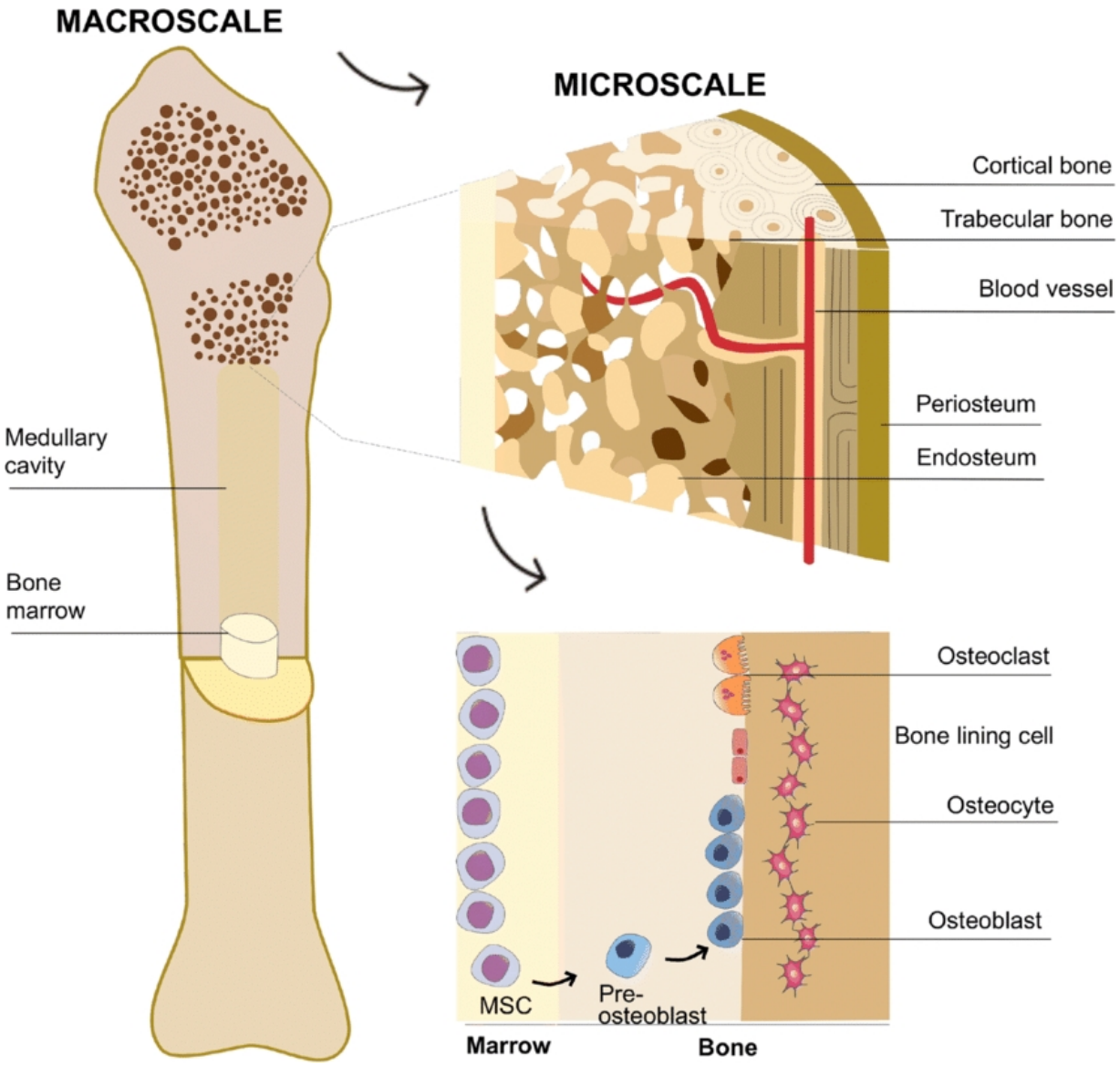

Fig.1-1 bone structure[6]

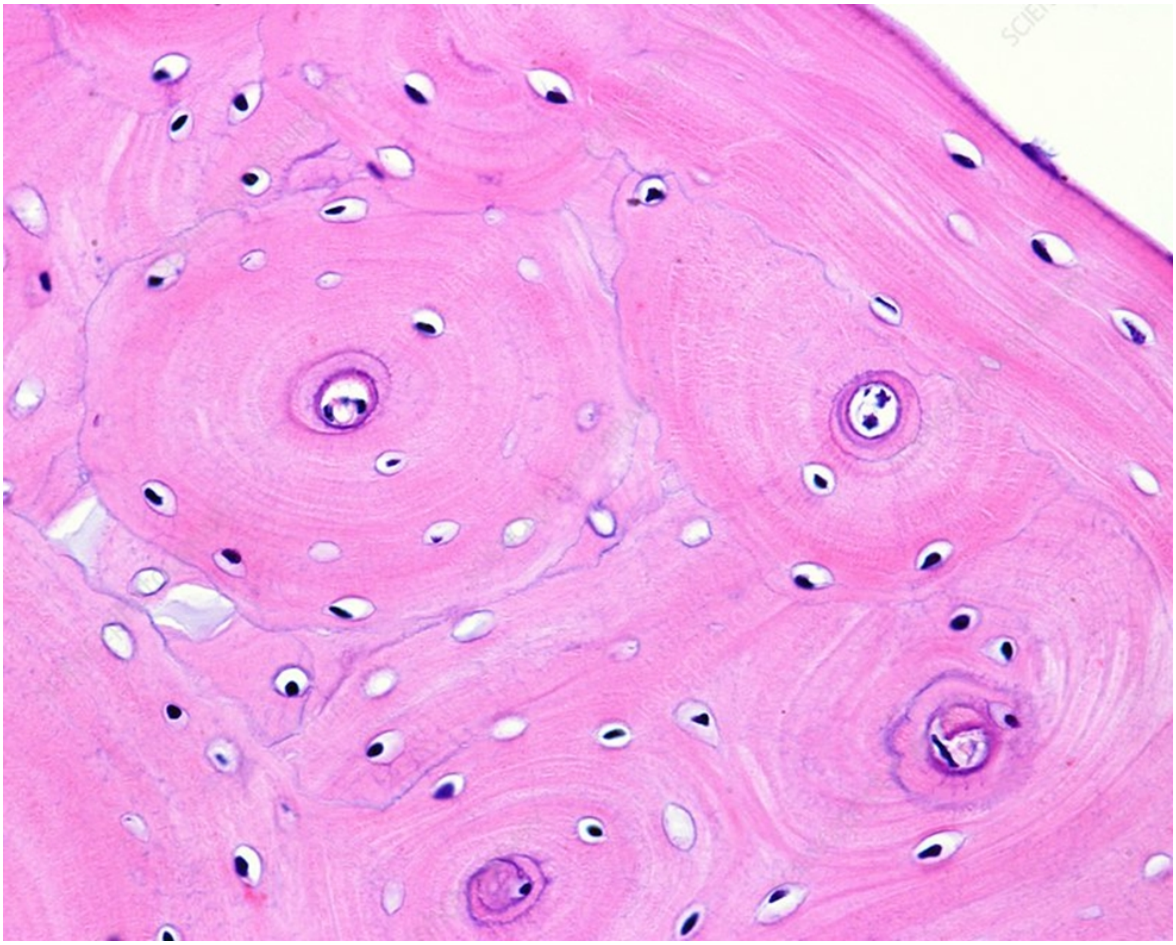

Fig.1-2 Cortical bone, light micrograph[7]

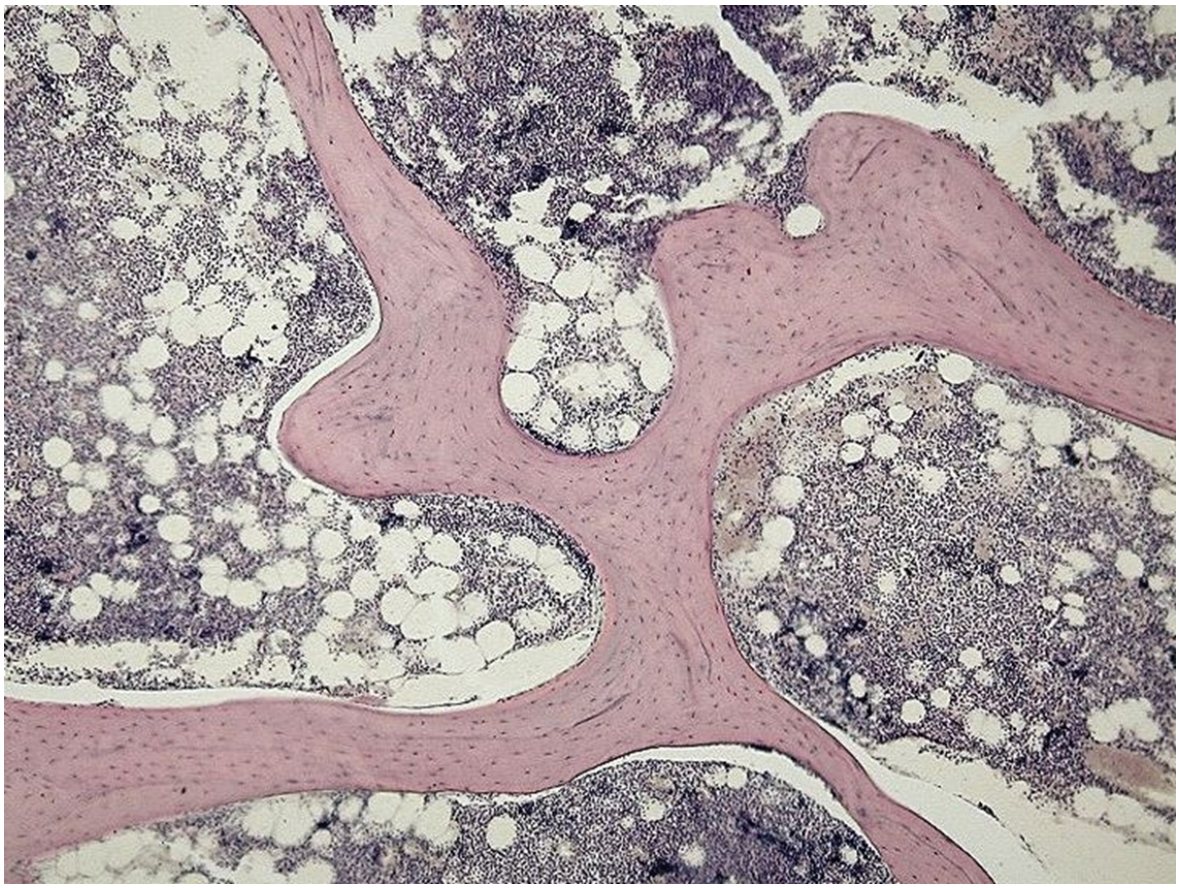

Fig.1-3 Micrograph of cancellous bone[8]

1.2 Mechanical parameters of bones

Young's modulus E, the Young’s modulus, or the modulus of elasticity in tension or compression (i.e., negative tension), is a mechanical property that measures the tensile or compressive stiffness of a solid material when the force is applied lengthwise. It quantifies the relationship between tensile/compressive stress sigma (force per unit area) and axial strain varepsilon (proportional deformation) in the linear elastic region of a material and is determined using the formula[9]:

$$E = \frac{\sigma}{\varepsilon} \qquad (1)$$

The Young's Modulus of a material is a fundamental property of every material that cannot be changed. It is dependent upon temperature and pressure however.

The Young's Modulus (or Elastic Modulus) is in essence the stiffness of a material. In other words, it is how easily it is bended or stretched.

Fig.1-4 is a stress-strain curve. The Young's modulus is the slope of the initial section of the curve.

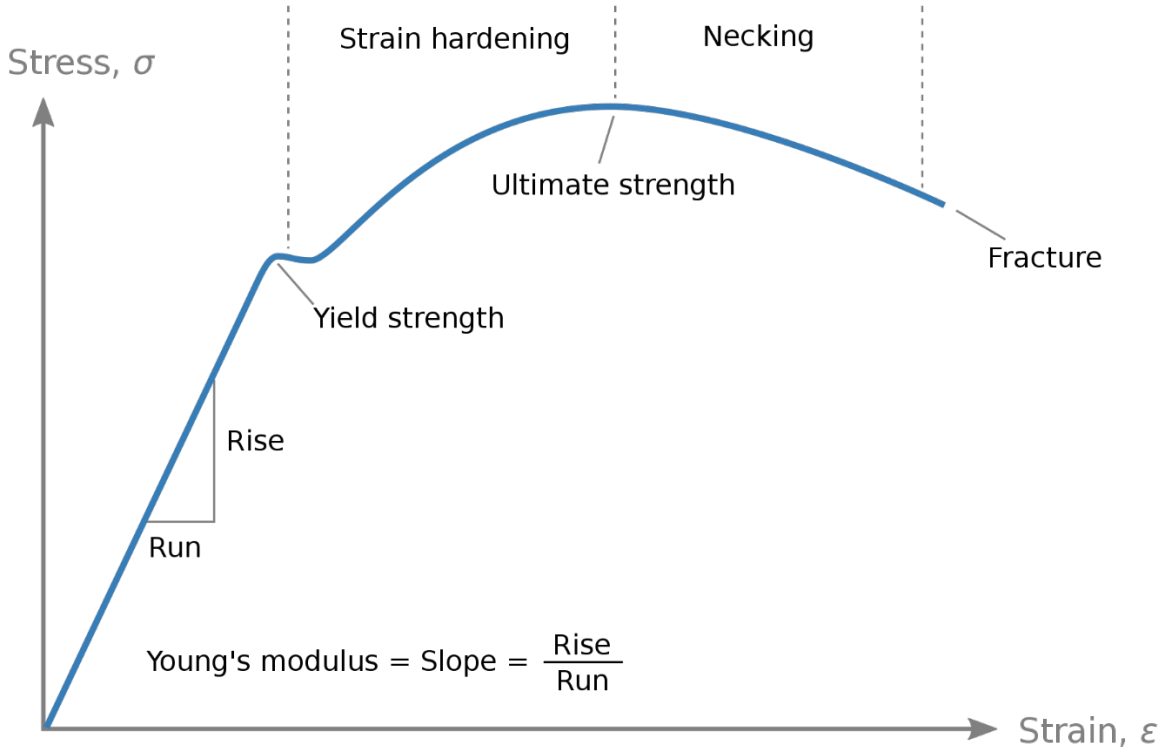

Fig.1-4 stress-strain curve[10]

1.3 Previous research

The mechanical properties of bone such as the elastic modulus E and the yield strength σ_y have been tried to be correlated with the bone mineral density (BMD) values such as the wet apparent density ρ_{app} and the ash density ρ_{ash}. In general, for example, the relations between E and ρ_{app} or ρ_{ash} can be expressed by an exponential function or linear function in which the parameters involved in the formulae are determined to fit experimental date best. On the contrary, development of the quantitative computed tomography (QCT) enables us to evaluate the BMD values of different bone parts of living patients, and such BMD obtained from QCT, ρ_{QCT}, has been utilized to assess osteoporosis clinically. Furthermore, the relationships between ρ_{QCT} and ρ_{ash} have been established experimentally and therefore, the formulae to express the relationships between E and ρ_{QCT} have been developed. Once the distributed mechanical properties of bone structures of a patient are determined by using QCT, the finite element method (FEM) is utilized to analyze the mechanical performance of the bone structures with three-dimensional bone models constructed using the CT-images and assigned properties in each of the finite elements. Thus, the accuracy of the computational results obtained by the CT-image based FEM (CT-FEM) is greatly relied upon the accuracy of estimation of the mechanical properties through QCT.

Exponential formulae to express E - ρ_{ash} relations were proposed by

Keyak[11][12] and Keller[13], independently.

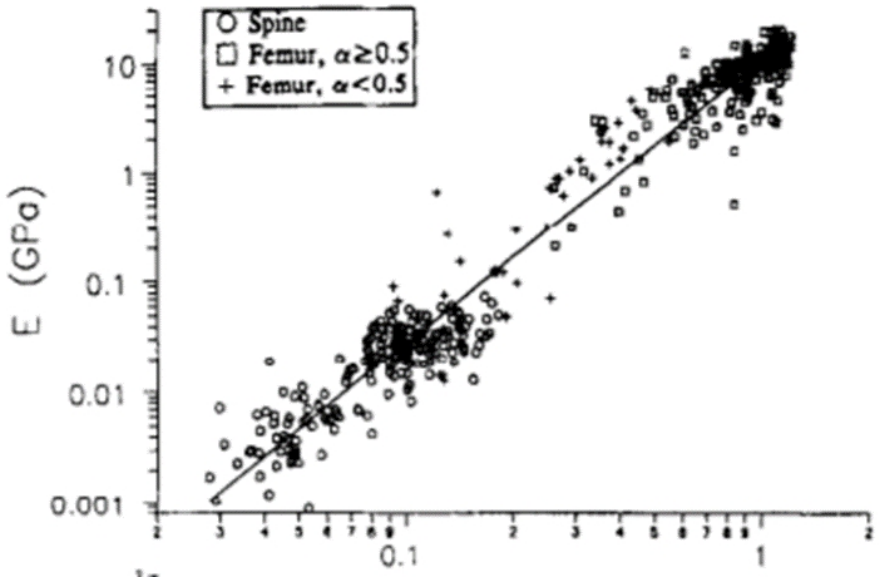

Fig.1-5 E - ρ_{ash} relations ,Kellar[13]

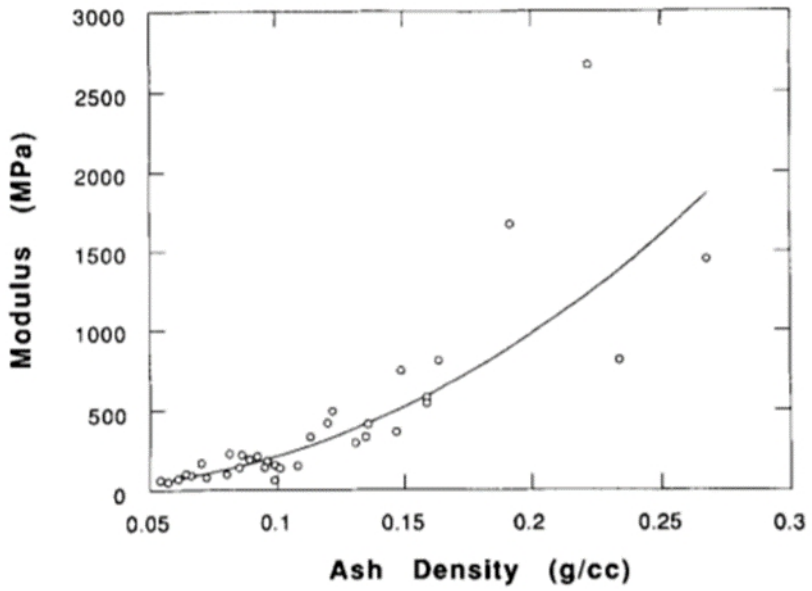

Fig.1-6 E - ρ_{ash} relations ,Keyak[11][12]

1.4 Objective of this research

The objective of this research is to explore the relationship between the elastic modulus of bone and its porosity and bone mineral density (BMD),and propose a macroscopic model that expresses the elastic modulus of bones as a function of BMD that based on previous research. Then, we revise the macroscopic model into microscopic model by the microstructure of bones. Finally, the microscopic model was used to calculate the elastic modulus of normal bones, bones with osteopenia and bone with osteoporotic, and compared with Keyak's experimental results to draw a conclusion.

2 Development of macroscopic model

2.1 Background

Understanding the mechanical properties of a material, particularly a material as complex as bone, requires a detailed knowledge of its structure. Bone, like most of the biologically formed materials, has a very complex hierarchical structure, which is not completely understood. Studies by Currey[14], however, show that the degree of mineralization and porosity are the two most important determinants of its mechanical properties.

The aim of this mathematical development is to express the elastic moduli of bone as a function of bone mineral density. A typical structure of bone can be divided into three regions, namely, cortical bone, trabecular bone (or cancellous bone) and bone marrow. In this theoretical modelling, a concept of poroelasticity with consideration of a representative volume element and the classical theory of composite materials is utilized to develop a model for the elastic modulus of cortical bone. On the contrary, the cubic strut model, a simple idealization of open-cell structure, is used to predict the elastic modulus of trabecular bone. It is assumed for bone marrow that its elastic modulus, E_{bm}, is a constant value.

2.2 Ideal poroelastic medium

A porous medium or a porous material is a material containing pores (voids). The skeletal portion of the material is often called the "matrix" or "frame". The pores are typically filled with a fluid (liquid or gas). The skeletal material is usually a solid, but structures like foams are often also usefully analyzed using concept of porous media.[15][16]

A porous medium is most often characterized by its porosity. Other properties of the medium (e.g., permeability, tensile strength, electrical conductivity, tortuosity) can sometimes be derived from the respective properties of its constituents (solid matrix and fluid) and the media porosity and pore's structure, but such a derivation is usually complex. Even the concept of porosity is only straightforward for a poroelastic medium.

Often both the solid matrix and the pore network (also known as the pore space) are continuous, so as to form two interpenetrating continua such as in a sponge. However, there is also a concept of closed porosity and effective porosity, i.e. the pore space accessible to flow.

An ideal poroelastic material is defined as a material in which two particular bulk moduli, $K'_s$and K''_s, are equal. The bulk modulus K'_s is defined as the change in the total medium volume per total medium volume when the entire medium is under a pressure regime in which the hydrostatic confining pressure is equal to the pore pressure, and the bulk modulus $K''_s$is defined as the change in total pore volume per total pore

volume under this pressure regime. For an ideal porous medium characterized by a fully connected pore space and by microscopically homogeneous and isotropic, chemically inert (solid and fluid) materials, it follows that $K_s = K'_s = K''_s$, where the notation $K_s$is the bulk modulus for the solid phase.[17][18]

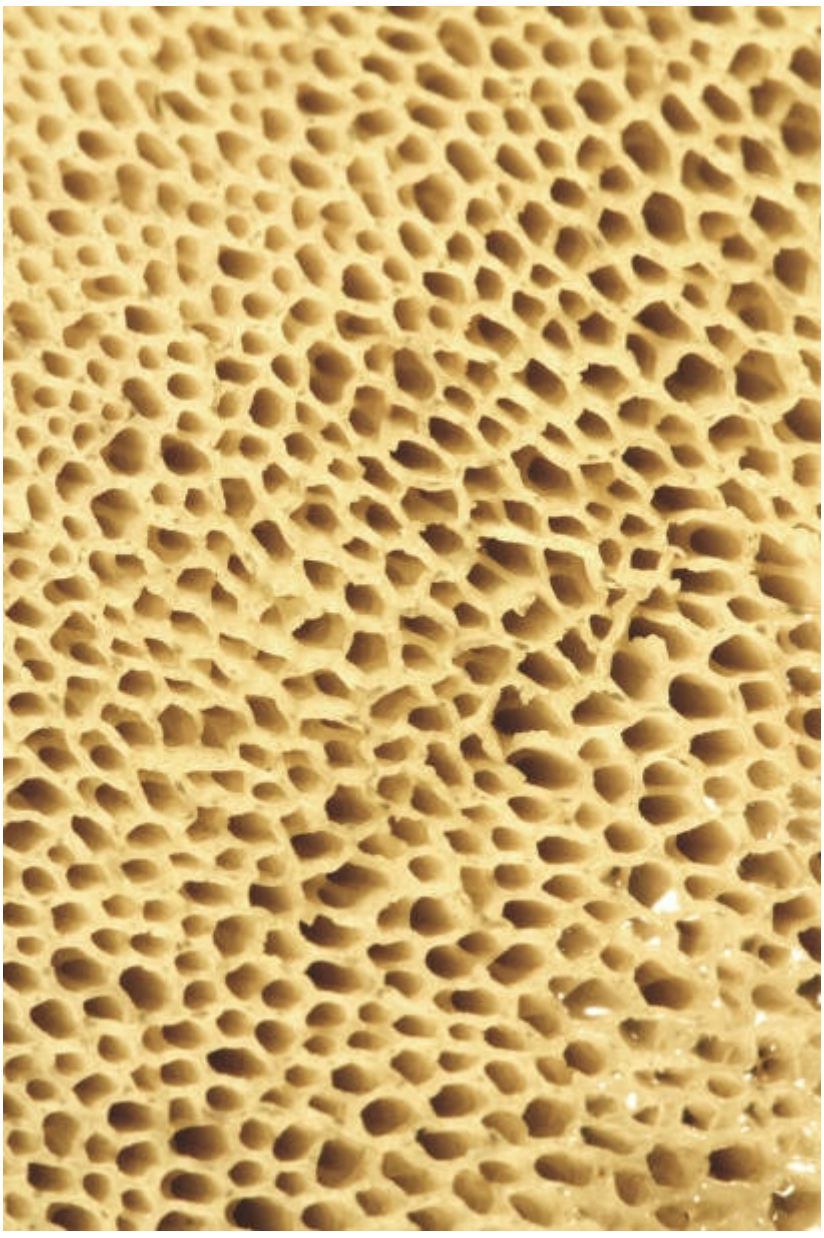

Fig.2-1 Porous structure of bone(19)

2.3 Elastic modulus of cortical bone

For an ideal poroelastic medium, the undrained bulk modulus, K_u, is given by[17][18]:

$$K_u = K\left[1+\frac{\alpha^2 K_f}{(1-\alpha)(\alpha-\phi_c)K_f+\phi_c K}\right] \quad (2)$$

where K is the bulk modulus of poroelastic medium under drained condition, K_f the bulk modulus of the fluid phase, ϕc the porosity of cortical bone and α,the effective stress coefficient and given by:

$$\alpha = 1-\frac{K}{K_s} \quad (3)$$

where K_s is the bulk modulus of the solid, i.e., bone tissue. The pores in cortical bone are assumed to be due to lacunar and canalicular. The bulk modulus K is also expressed as a function of ϕc such that:

$$K = K_s\left[1-\left(\frac{3K_s}{4G_s}+1\right)\phi_c\right] \quad (4)$$

where G_s is the shear modulus of the solid. Substituting the following relations for elastic medium:

$$K = \frac{E}{3(1-2\nu)} \quad (5)$$

$$K_u = \frac{E_u}{3(1-2\nu_u)} \quad (6)$$

$$K_s = \frac{E_s}{3(1-2\nu_s)} \quad (7)$$

$$K_f = \frac{E_f}{3(1-2\nu_f)} \quad (8)$$

$$G_s = \frac{E_s}{2(1+\nu_s)} \quad (9)$$

where ν, νu, νs, νf are the corresponding Poisson's ratios into Eqs. (2)-(9),we obtain

$$E_u = E\left(\frac{1-2\nu_u}{1-2\nu}\right)\left[1+\frac{(1-2\nu)\alpha^2 E_f}{(1-2\nu)(1-\alpha)(\alpha-\phi_c)E_f+(1-2\nu_f)\phi_c E}\right] \quad (10)$$

$$\alpha = 1-\frac{(1-2\nu_s)E}{(1-2\nu)E_s} \quad (11)$$

$$E = E_s\left(\frac{1-2\nu}{1-2\nu_s}\right)\left[1-\left(\frac{1+\nu_s}{2(1-2\nu_s)}+1\right)\phi_c\right] \quad (12)$$

The elastic modulus, E_c, of cancellous bone is assumed to be identical with the undrained elastic modulus, E_u. By assuming $\nu_s = \nu_u = \nu = \nu_f$ and substituting Eqs. (11) and (12) into (10), one can obtain:

$$E_c = E_s A\left[1+\frac{BE_f}{CE_f+DE_s}\right] \quad (13)$$

Where

$$A(\phi_c) = 1-\frac{3(1-\nu_s)}{2(1-2\nu_s)}\phi_c \quad (14)$$

$$B(\phi_c) = 9(1-\nu_s)^2\phi_c^2 \quad (15)$$

$$C(\phi_c) = 2(1+\nu_s)(1-2\nu_s)-3(1-\nu_s^2)\phi_c \quad (16)$$

$$D(\phi_c) = 4(1-2\nu_s)^2\phi_c-6(1-\nu_s)(1-2\nu_s)\phi_c^2 \quad (17)$$

2.4 Elastic modulus of trabecular bone

The porous structure of trabecular bone is modelled as the cubic strut model which corresponds to a lattice structure shown in Fig.2-2[20][21]. The struts correspond to trabecular and the continuous porous region is assumed to be filled with bone marrow. The representative unit cell can be constructed as shown in Fig.2-3. The compressive deformation behavior of the unit cell under a small fixed displacement condition, Δu, can be analyzed by linear elasticity by considering three subdivisions A, B, and C shown in Fig.2-4.

The stress-strain relations are given by:

$$\sigma_A = E_{bm}\varepsilon \quad (18)$$

$$\sigma_B = E_s\varepsilon \quad (19)$$

$$\sigma_C = \frac{E_s E_{bm}}{E_s + (E_{bm} - E_s)\beta}\varepsilon \quad (20)$$

$$\beta = \frac{l}{L} \quad (21)$$

$$\varepsilon = \frac{\Delta u}{L} \quad (22)$$

where $\sigma_A, \sigma_B, \sigma_C$ are the compressive stress generated in A, B, and C. E_s and E_{bm} are the elastic moduli of trabecula, i.e., bone tissue and bone marrow filled in the pores, respectively. The total force is therefore given by:

$$\begin{aligned} F &= 4\sigma_A\left(\frac{L-l}{2}\right)^2 + \sigma_B l^2 + 4\sigma_C l\left(\frac{L-l}{2}\right) \\ &= \left[E_s l^2 + E_{bm}(L-l)^2 + \frac{2E_s E_{bm}}{E_s + (E_{bm}-E_s)\beta} l(L-l)\right]\varepsilon \end{aligned} \quad (23)$$

Therefore, the relation between the average stress, σ_m, and the strain is expressed by:

$$\sigma_m = \frac{F}{L^2} = \left[E_s\beta^2 + E_{bm}(1-\beta)^2 + \frac{2E_s E_{bm}\beta(1-\beta)}{E_s + (E_{bm}-E_s)\beta}\right]\varepsilon \quad (24)$$

On the other hand, the porosity (or the volume fraction of the bone marrow) is given by

$$\phi_t = 1 - \left(\frac{l}{L}\right)^2\left(3 - 2\frac{l}{L}\right) = 1 - \beta^2(3-2\beta) \quad (25)$$

Then the effective elastic modulus of the unit cell is given by:

$$E_t = \frac{\sigma_m}{\varepsilon} = E_s\beta^2 + E_{bm}(1-\beta)^2 + \frac{2E_s E_{bm}\beta(1-\beta)}{E_s + (E_{bm}-E_s)\beta} \quad (26)$$

And

$$\phi_t = 2\beta^3 - 3\beta^2 + 1 \quad (27)$$

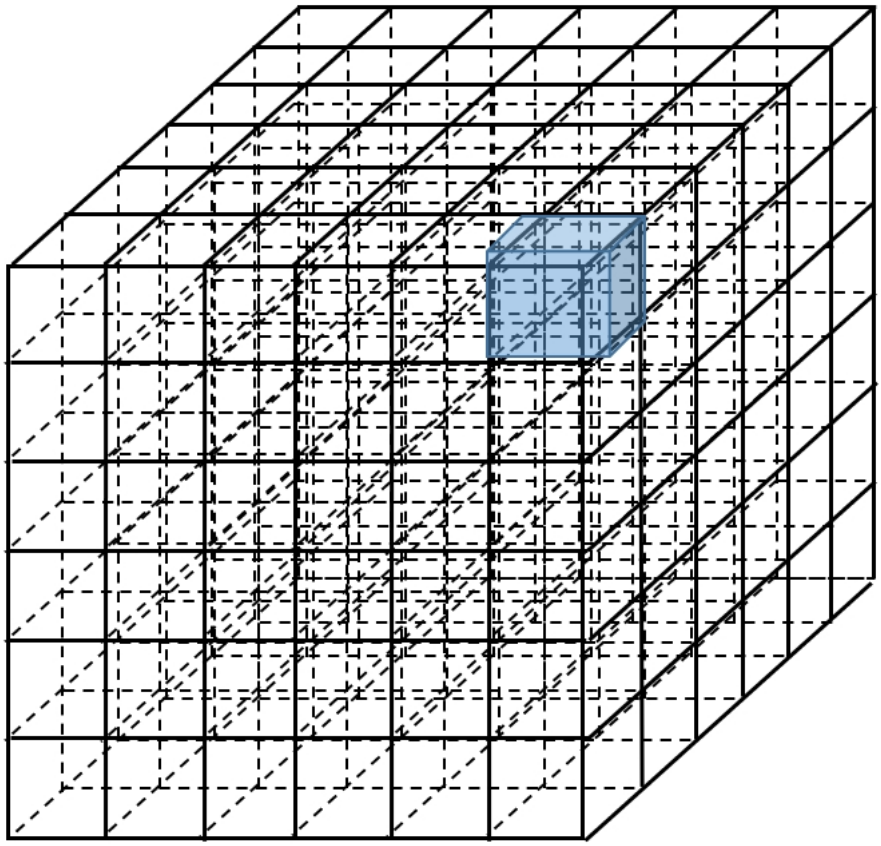

Fig.2-2 Lattice structure model for the porous structure of trabecular bone

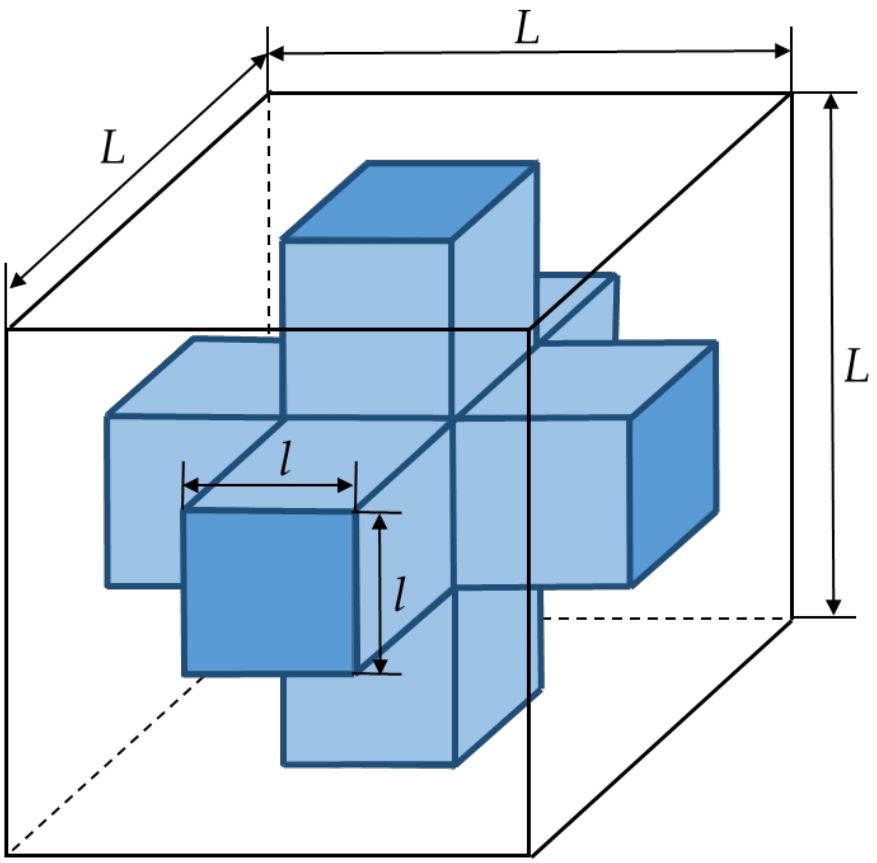

Fig.2-3 The representative unit cell

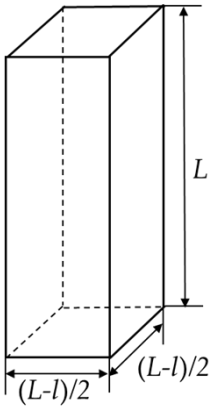

Subdivision A

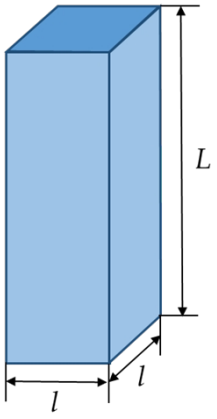

Subdivision B

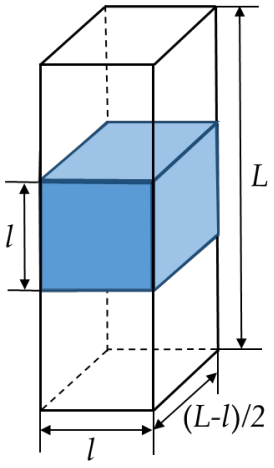

Subdivision C

Fig.2-4 Three subdivisions of the unit cell

2.5 Results and discussion

In the above, we have obtained the equations of E_c(the Young's modulus of cortical bones) and E_t(the Young's modulus trabecular bones) as Eqs.(13)(14)(15)(16)(17)and Eqs.(26)(27). According to literature review, $E_s >> E_f$ while $E_s >> E_{bm}$, so the equations of E_c and E_t can be simplified to

$$E_c = E_s(1 - \frac{3(1-v_s)}{2(1-2v_s)})\phi_c \quad (28)$$

and

$$E_t = E_s\beta^2 \quad (29)$$

while

$$\phi_t = 2\beta^3 - 3\beta^2 + 1 \quad (30)$$

Some parameters were determined by following references: E_s=14GPa, v_s=0.3, $0 < \phi_c < 0.2$, $0.2 < \phi_t < 0.9$[17]. In the theory, BMD(ρ)=1-ϕ. Substituting the above data into the equation to calculate, we can get the Eqs.(31) and Table 2-1. Combining the above calculation results with the Keyak's empirical formulae in Table 2-2[11,12,22], Fig.2-5 can be obtained.

Table 2-1 Calculated data under the macroscopic model

BMD(g/cm³)	E(GPa)
0.8	7.12
0.75	6.36
0.7	5.68
0.65	5.06
0.6	4.50
0.55	3.98
0.5	3.50
0.45	3.05
0.4	2.62
0.35	2.23
0.3	1.84
0.25	1.49
0.2	1.15
0.15	0.83
0.1	0.54

$$E=14(2.625BMD-1.625)\quad(BMD>0.8)\quad(31)$$

Table 2-2 Keyak's empirical formulae [11,12,22]

Density Range(g/cm^3)	Elastic Modulus (GPa)
$\rho=0$	$E=0.001$
$0<\rho \leqq 0.27$	$E=33.900\rho^{2.20}$
$0.27<\rho<0.6$	$E=5.307\rho+0.469$
$\rho \geqq 0.6$	$E=10.200\rho^{2.01}$

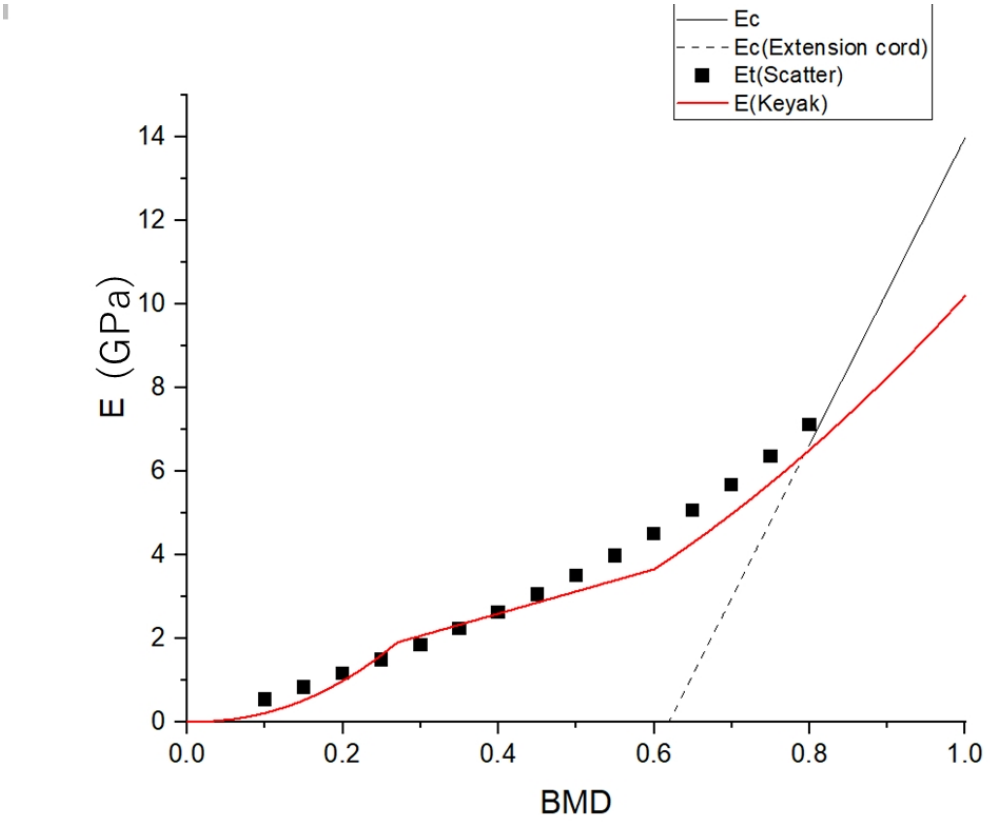

Fig.2-5 Variation of Young's modulus (E) with BMD from macroscopic model

According to Fig.2-5, in this study, the change trend of the results calculated by the macroscopic model is basically consistent with Keyak's model, but the overall value is higher than Keyak's results. The reason for it is the Es is not a fixed value as we set when performing macroscopic model calculations.

2.6 Summary

In this phase, we proposed a macroscopic model that expresses the elastic modulus of bones as a function of BMD that based on previous research and used it to calculate some results. We find that the change trend of the results calculated by the macroscopic model is basically consistent with Keyak's model, but the overall value is higher than Keyak's results. The reason for it is the E_s is not a fixed value as we set when performing macroscopic model calculations. In fact, the value of Es will be affected by the microstructure of the bone, such as the loading angle. In the next part of the study, we will use this to correct the macroscopic model.

3 Development of microscopic model

3.1 Bone tissue

As above, the studies by Currey[14], however, show that the degree of mineralization and porosity are the two most important determinants of bones' mechanical properties. This implies that the structure of bone at the level of crystal organization is of particular importance in understanding its mechanical properties. Thus, modeling bone's mechanical properties requires detailed structural information on crystal shapes and sizes, and on their orientations and organization relative to the collagen framework. It should also include information on the structural differences between lamellae, as well as the organization of lamellae into even larger cylindrical-shaped structures, called the osteons or the Haversian systems.

The bone tissue can be recognized as a composite material of organic and inorganic materials. The typical components of the organic and inorganic phases are collagen and carbonate apatite. Therefore, the mechanical models of bone tissue have been developed on the basis of two phase composite material. In the present study, a multi-scale composite model developed by Wager and Weiner[23,24] is used to obtain the elastic modulus, E_s, of bone tissue. The representative volume element of a bone tissue is considered to be constructed by a three-layer structure of lamellae as shown in Fig.3-1, in which a thick lamellae of about 3μm thick is sandwiched between thin lamellae of about 0.3μm thick. Each of lamellae is assumed to be a collagen-crystal composite in

which rectangular crystal plates of carbonate apatite are arranged in parallel layers within collagen fibrils. Therefore, the mechanical formula developed for platelet-reinforced composites may be utilized to express the properties of the lamellae.

Attempts to model bone are always limited by the state of understanding of bone structure. Currey considered bone as a two-phase composite material. Using the theoretical scheme of Cox[25],Currey[26,27] quantified the dependence of the longitudinal Young's modulus of bone on the basic concept of cylindrically shaped apatite crystals embedded in a collagen matrix and aligned with the long axis of collagen fibrils. Lang[28] and Reilly and Burstein[29] considered bone to be a transversally isotropic material, the stiffness behavior of which could be fully described by five independent constants.

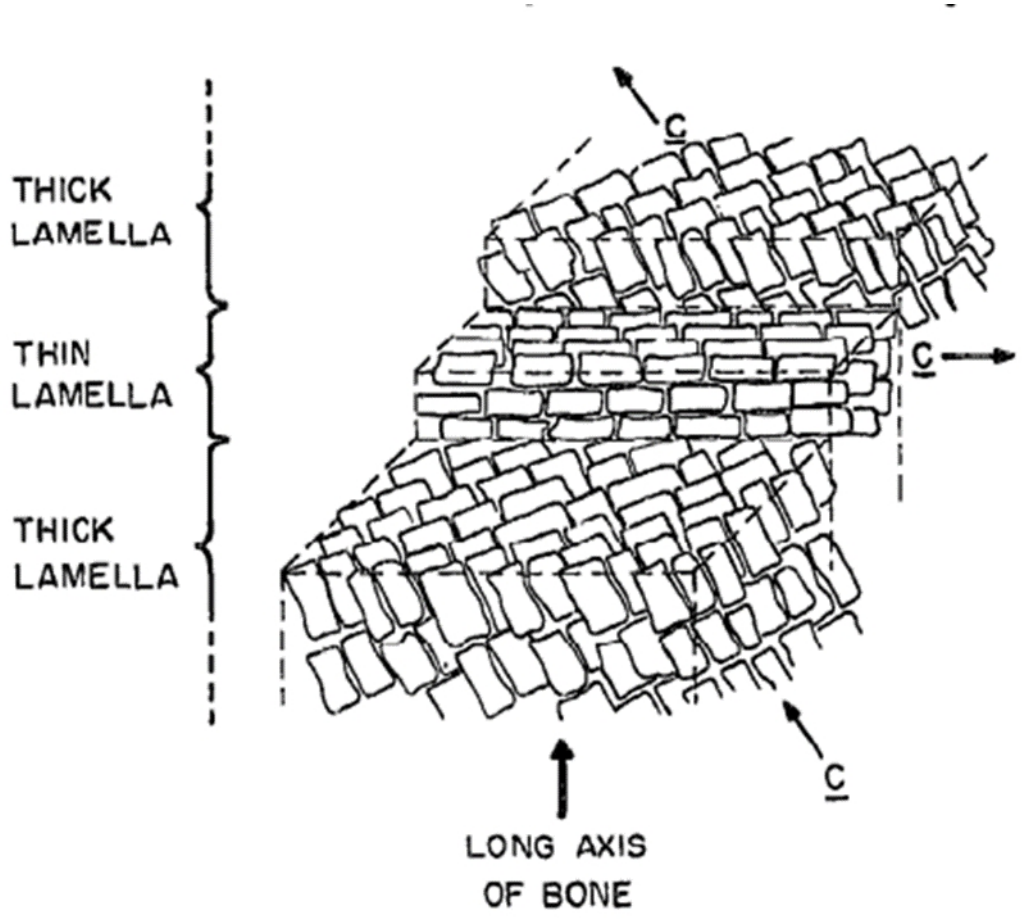

Fig.3-1 Bones microstructure [23,24]

3.2 Modifications to the model

By the Currey[27]and Reilly and Burstein's[29] theory, the anisotropic elastic modulus of bone can be expressed as a function of the loading angle,θ, which is taken as 0° parallel to the longitudinal axis of bone and 90° perpendicular to it. The function can be written as:

$$E(\theta)=\left[\frac{\cos^4\theta}{E_1}+\frac{\sin^4\theta}{E_2}+\left(\frac{1}{G_{12}}-2\frac{\nu_{12}}{E_1}\right)\sin^2\theta\cos^2\theta\right]^{-1} \quad (32)$$

E_1 and E_2 are the longitudinal(parallel to the long axis of bone) and transverse Young's moduli of bone, respectively, and G_{12} and v_{12} are the longitudinal-transverse shear modulus and Poisson ratio of bone, respectively[30].

It is then assumed that the anisotropic elastic moduli of the lamellae structures are also able to be expressed by Eqs.(32). From microstructural point of view, it is simply assumed that the angles between the longitudinal direction of the thin and thick lamellae and the long axis of bone are θ_{thin} and θ_{thick}, respectively. Therefore, the elastic moduli of the thin and the thick lamellae, E_{thin} and E_{thick}, are expressed using Eqs.(32) such that:

$$E_{thin}(\theta)=\left[\frac{\cos^4(\theta+\theta_{thin})}{E_1}+\frac{\sin^4(\theta+\theta_{thin})}{E_2}+\left(\frac{1}{G_{12}}-2\frac{\nu_{12}}{E_1}\right)\sin^2(\theta+\theta_{thin})\cos^2(\theta+\theta_{thin})\right]^{-1} \quad (33)$$

$$E_{thick}(\theta)=\left[\frac{\cos^4(\theta+\theta_{thick})}{E_1}+\frac{\sin^4(\theta+\theta_{thick})}{E_2}+\left(\frac{1}{G_{12}}-2\frac{\nu_{12}}{E_1}\right)\sin^2(\theta+\theta_{thick})\cos^2(\theta+\theta_{thick})\right]^{-1} \quad (34)$$

where θ_{thin} and θ_{thick} are the angles between the longitudinal direction of the thin and thick lamellae and the long axis of bone.

Using the rule of mixture, the elastic modulus, E_s, of the representative element for bone tissue is given as a function of θ,such that:

$$E_s(\theta) = V_{thin}E_{thin}(\theta) + V_{thick}E_{thick}(\theta) \quad \text{with} \quad V_{thin} + V_{thick} = 1 \qquad (35)$$

Where V_{thin} and V_{thick} are the volume fractions of thin and thick lamellae.

Although the range of the anisotropic elastic modulus of mature bovine bone is from 10 to 18 GPa , for simplicity, the average modulus, $\overline{E}_s$, defined by:

$$\overline{E}_s = \frac{2}{\pi}\int_0^{\pi/2} E_s(\theta)\,d\theta = \frac{2}{\pi}\int_0^{\pi/2}\left[V_{thin}E_{thin}(\theta) + V_{thick}E_{thick}(\theta)\right]d\theta \qquad (36)$$

is used as the value of E_s in this study, and therefore

$$E_s = \frac{2}{\pi}\int_0^{\pi/2}\left[V_{thin}E_{thin}(\theta) + V_{thick}E_{thick}(\theta)\right]d\theta \qquad (37)$$

3.3 Determination of some parameters

The shear modulus G_{12} of a single lamella is given by the Halpin-Tsain equation[31,32]:

$$G_{12} = G_m\left(\frac{1+2\alpha_1\eta_1\phi_p}{1-\eta_1\phi_p}\right) \quad (38)$$

with

$$\eta_1 = \frac{G_p/G_m - 1}{G_p/G_m + 2\alpha_1} \quad (39)$$

where α_1 is the ratio of the platelet width to thickness, ϕ_p ,the volume fraction of the platelets, and G_m, the shear modulus of the matrix.

The Poisson's ratio of a single lamella is assumed to be given by the rule of mixture[31,32]:

$$\nu_{12} = \nu_p\phi_p + \nu_m(1-\phi_p) \quad (40)$$

Where ν_p is the Poisson's ratio of the platelets and ν_m,the Poisson's ratio of the matrix.

3.4 Three different models for E_1 and E_2

The structure of the collagen-crystal composite that makes up an individual lamella clearly shows that it should be modeled as a platelet-reinforced composite, rather than a fiber-reinforced composite. Very few theoretical or experimental studies have been made on the elastic properties of platelet-reinforced composites, apart from a result proposed by Halpin and Tsai[31.33], a theoretical model by Padawer and Beecher[34], and a model by Lusis [35]. (These are here termed as the HT, PB and LWX models.) These models are similar to that of Cox[25], but they take into account the platelet-like geometry of the reinforcement. Jackson[36] have studied the mechanical design of mollusk shell nacre viewed as a composite reinforced with platelets rather than with fibers, and a similar view is adopted here for bone.

According to the Halpin-Tsain equations, the longitudinal modulus of a lamella reinforced with rectangular crystals oriented as in the thin lamellae in Fig.3-1 is given by

$$E_1 = E_m\left(\frac{1 + 2\alpha_1\eta_1\phi_p}{1 - \eta_1\phi_p}\right) \qquad (41)$$

with

$$\eta_1 = \frac{Ep/Em - 1}{Ep/Em + 2\alpha_1} \qquad (42)$$

where E_p, E_m are the elastic moduli of the apatite platelets and the collagen matrix and α_1, the ratio of the platelet width to thickness. The transverse elastic modulus, E_2,

is given by the same expression as E_1, but with α_2 instead of α_1,where α_2 is the ratio of the platelet length to thickness, and η_1 is replaced by η_2.

Both the Padawer and Beecher's and the Lusis's models propose similar expressions for the longitudinal modulus, E_1, and the transverse modulus, E_2, with slight differences as follows:

$$E_1 = \varsigma E_p \phi_p + E_m(1-\phi_p) \qquad (43)$$

In which, for the Padawer and Beecher's model,the modulus reduction factor, ς, is given by

$$\varsigma = 1 - \frac{\tanh \gamma}{\gamma} \qquad (44)$$

Whereas for Lusis's model,

$$\varsigma = 1 - \ln \frac{\gamma + 1}{\gamma} \qquad (45)$$

In both cases,

$$\gamma = \alpha_1 \left(\frac{\phi_p}{1-\phi_p} \right)^{1/2} \left[\frac{G_m}{E_p} \right]^{1/2} \qquad (46)$$

The transverse elastic modulus, E_2, is given by the same expression as E_1, but with α_2 instead of α_1.

The LWX scheme is essentially a modified version of the PB model, as it takes into account platelet-platelet interactions at high platelet content. For the experimental data of the two models, for example , glass, aluminum diboride and silicon carbide platelets

in PB and phlogopite and muscovite mica flakes in LWX, we can find that most experimental data fall short of all schemes due to variability in the geometrical and the structural parameters, but the general trends are quite satisfactory. Thus, three different expressions for both E_1 and E_2, can be used to model a single bone lamella. But it's worth noting that, water, a major constituent of bone, is not taken into account as it probably contributes little to the Young's modulus.

3.5 Results and discussion

Based on previous readings, It is assumed that the apatite platelets have aspect ratios of α_1=10 and α_2=25[23], and that the experimental stiffness constants of both the apatite platelets and the collagen matrix are:

Table 3-1 Some parameters determined by references

Variable	Value
α_1&α_2	10 & 25 [23]
E_p	114.0GPa [37]
E_m	1.5GPa [27]
G_p	44.5GPa [37]
G_m	1.0GPa [38]
ϕ_p	0.35 [39]
ν_p	0.3 [39]
v_{12}	0.35 [39]
V_{thin}	0.8 [40]
V_{thick}	0.2 [40]
θ_{thin}	0° [40]
θ_{thick}	63° [40]

Bring the values of the above variables into the Eqs.(33)to(46), and calculate

through the HT, PB and LWX models respectively to get Table 3-2.

Table 3-2 The value of Es varying with θ

Angle(°)	Es(HT)(GPa)	Es(PB) (GPa)	Es(LWX)(GPa)
0	13.160	9.702	9.864
5	13.070	9.600	9.866
10	13.144	9.604	9.760
15	13.382	9.766	9.746
20	13.746	10.190	9.998
25	14.176	10.948	10.636
27	14.342	11.356	11.024
30	14.572	12.090	11.756
35	14.844	13.688	13.484
40	14.890	15.750	15.934
45	14.698	18.130	19.134
50	14.286	20.508	22.834
55	13.732	22.312	25.224
60	13.156	23.060	28.264
65	12.608	22.628	28.236
70	12.134	21.372	26.634

75	11.664	19.950	24.470
80	11.396	18.624	22.516
85	11.144	17.666	21.174
90	10.988	17.164	20.546

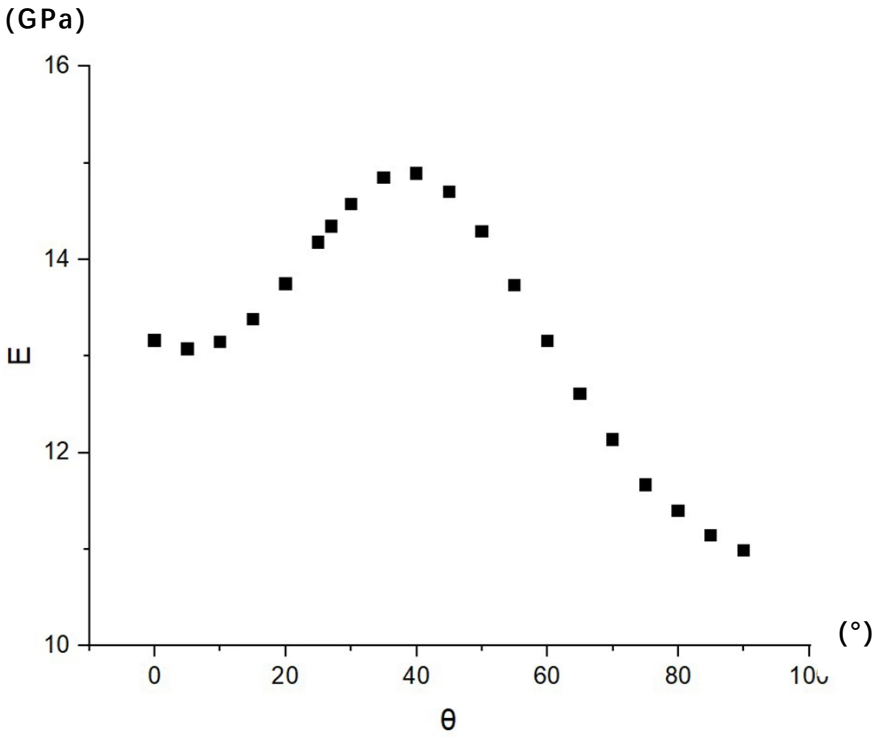

Fig.3-2 Variation of Young's modulus of bone as calculated from the HT model

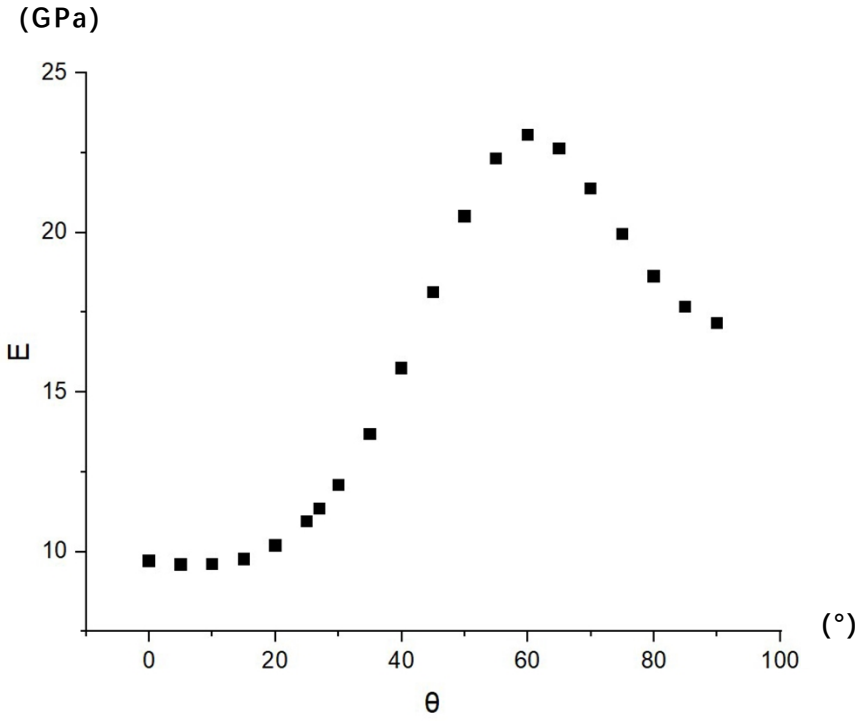

Fig.3-3 Variation of Young's modulus of bone as calculated from the PB model

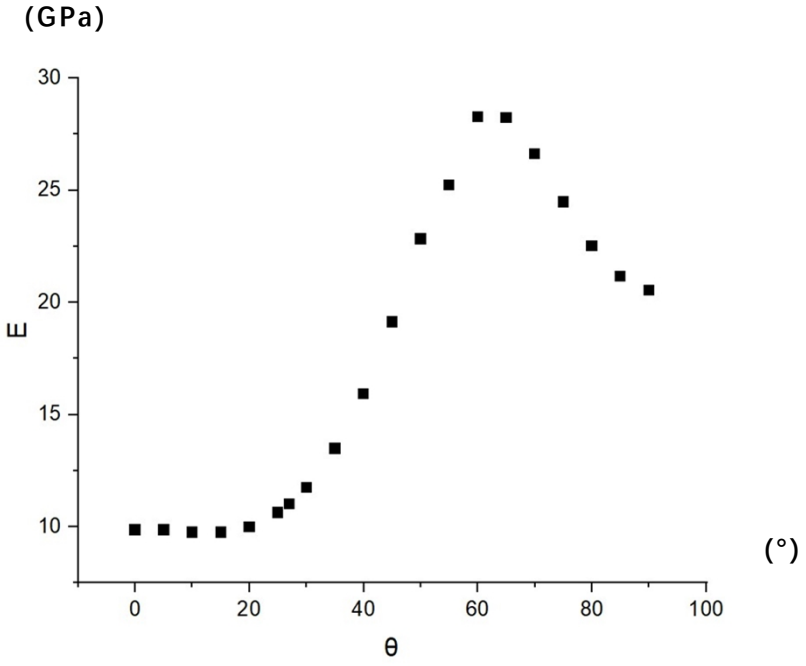

Fig.3-4 Variation of Young's modulus of bone as calculated from the LWX model

According to the Table 3-1,the Fig.3-2,3-3 and 3-4,it can be calculated that:

Es(HT)=13.257GPa

Es(PB)=15.705GPa

Es(LWX)=17.530GPa

Comparing the results of this calculation with the previous studies reviewed, we find that Young's modulus of bone vs the loading angle shows trends similar to the experimental data of Bonfield and Grynpas[41] for the PB model, and the Es value calculated by the HT model is closer to the experimental results. For the LWX model, in this study, its numerical change trend and final calculation results are inconsistent with the previous experimental data, so it will be discarded in the next part of the study.

3.6 Summary

In this phase, we revised the macroscopic model into microscopic model by the microstructure of bones, added consideration of the impact of loading angle on the value of E_s. In order to specifically calculate the impact of loading angle on E_s, for the two important paraments in the functions - E_1 and E_2, when determining their values, we used three different theoretical models - HT model, PB model and LWX model. Comparing the results of the calculation of E_s in three models with the previous studies reviewed, we find that Young's modulus of bone vs the loading angle shows trends similar to the experimental data of Bonfield and Grynpas[41] for the PB model, and the Es value calculated by the HT model is closer to the experimental results. For the LWX model, in this study, its numerical change trend and final calculation results are inconsistent with the previous experimental data, so only the HT and PB models will be used for the next part of the calculation.

4 Application of microscopic model

4.1 Osteopenia and Osteoporosis

Osteoporosis is a systemic skeletal disorder characterized by low bone mass, micro-architectural deterioration of bone tissue leading to bone fragility, and consequent increase in fracture risk. It is the most common reason for a broken bone among the elderly[42].

Osteoporosis itself includes three broad categories of symptoms:

(1) Pain. Patients may have low back pain or body pain. When the load increases, the pain will aggravate or the activity will be limited. In severe cases, it will be difficult to turn over, sit up and walk.

(2) Spine deformation. People with severe osteoporosis may have shortened height and hunchback. Vertebral compression fractures can lead to thoracic deformity, abdominal compression, and affect cardiopulmonary function.

(3) Fracture. Fractures that occur without trauma or minor trauma are fragility fractures. Bones may weaken to such a degree that a break may occur with minor stress or spontaneously. Common sites of fragility fractures are the thoracic and lumbar spine, hip, radius, distal ulna, and proximal humerus. After the broken bone heals, the person may have chronic pain and a decreased ability to carry out normal activities.[43]

Osteopenia, known as "low bone mass" or "low bone density", is a condition in which bone mineral density is low. Because their bones are weaker, people with

osteopenia may have a higher risk of fractures, and some people may go on to develop osteoporosis.[44] In 2010, 43 million older adults in the US had osteopenia.[45] Unlike osteoporosis, osteopenia does not usually cause symptoms, and losing bone density in itself does not cause pain.

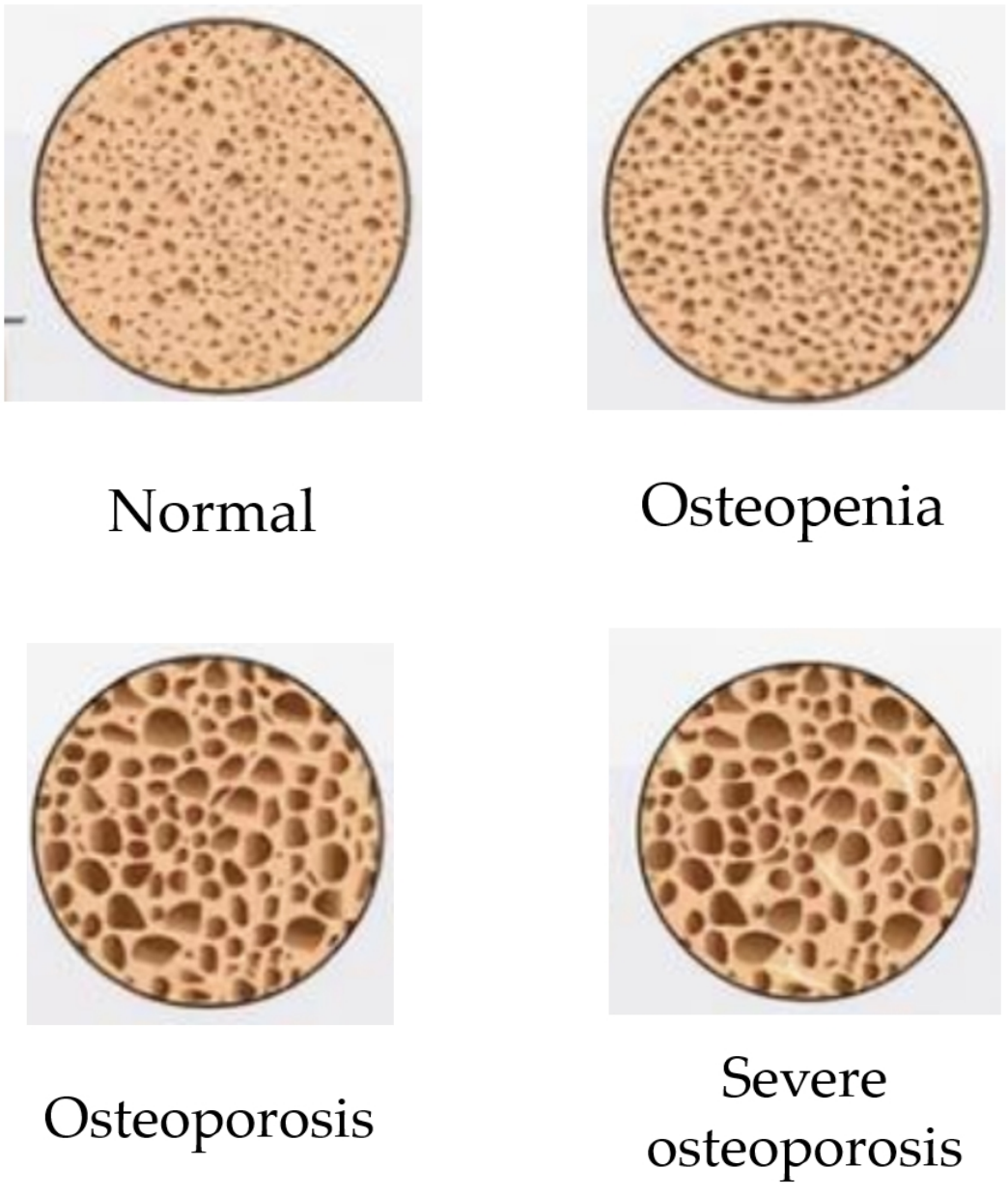

Fig.4-1 Models of bones in different states[46]

4.2 Diagnostic guidelines for osteoporosis

Osteoporosis can be diagnosed using conventional radiography and by measuring the bone mineral density (BMD).The most popular method of measuring BMD is dual-energy X-ray absorptiometry.

Dual-energy X-ray absorptiometry (DXA, or DEXA)[47] is a means of measuring bone mineral density (BMD) using spectral imaging. Two X-ray beams, with different energy levels, are aimed at the patient's bones. When soft tissue absorption is subtracted out, the bone mineral density (BMD) can be determined from the absorption of each beam by bone. Dual-energy X-ray absorptiometry is the most widely used and most thoroughly studied bone density measurement technology.

In the test of DXA scan, two indicators can be obtained: Z-score and T-score. The Z-score is the number of standard deviations (SD) above or below the mean for the patient's age, sex and ethnicity and the T-score means the number of standard deviations above or below the mean for a healthy 30-year-old adult of the same sex and ethnicity as the patient. The previous researches show that the Z-score is age dependent, while the T-score is age independent. The World Health Organization (WHO) has established the diagnostic guidelines which in Table 4-1.[48][49]

As described in Table 4-2, a different set of guidelines than the WHO guidelines was used to diagnose osteoporosis in Japan, where the YAM means young adult mean (20–44 years old for lumbar spine, 20–29 years old for proximal femur), and the SD

means normal adult bone density standard deviation.[50]

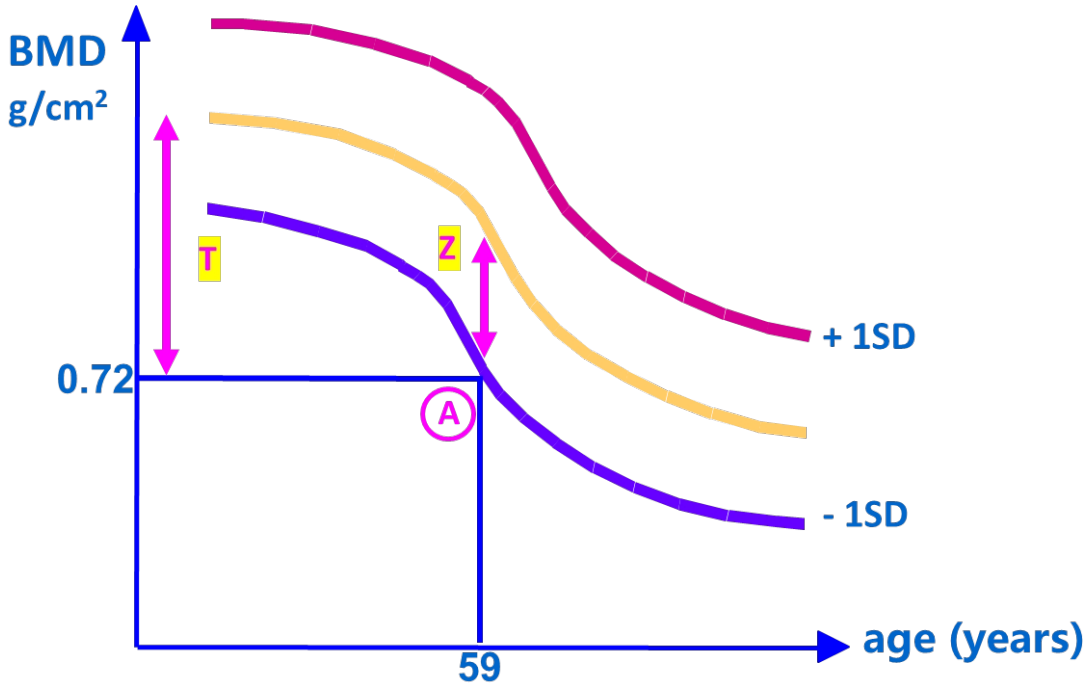

Fig.4-2 Examples of T-scores and Z-scores[51]

(Z-score:-1.0　T-score:-2.5)

Table 4-1 Diagnostic guidelines for osteoporosis recommended by WHO [48][49]

Category	T-score range
Normal	T-score ≥ −1.0
Osteopenia	−2.5 < T-score < −1.0
Osteoporosis	T-score ≤ −2.5
Severe osteoporosis	T-score ≤ −2.5 with fragility fracture

Table 4-2 Diagnostic guidelines for osteoporosis recommended in Japan [50]

<table>
<tr><td>Category</td><td colspan="2">State of the bones</td></tr>
<tr><td>Osteopenia</td><td colspan="2">Bone density greater than -2.5 SD and less than -1.0 SD</td></tr>
<tr><td rowspan="3">Osteoporosis</td><td rowspan="2">With fragility fracture</td><td>Vertebral fracture or hip fracture</td></tr>
<tr><td>Other fragility fractures and bone density <80% of YAM</td></tr>
<tr><td>Without fragility fracture</td><td>Bone density ≤70% of YAM or -2.5 SD</td></tr>
</table>

4.3 **Results and discussion**

In the calculation at this stage, the values of other parameters except E_p and G_p are the same as those in Table 3-1, while the E_p and G_p of different bones and the E_s values calculated by them through the HT model and the PB model respectively given in Table 4-3.

Table 4-3 E_p,G_p for different kind of bones and the value of E_s calculated by HT and PB models

	Normal	Osteopenia	Osteoporosis
E_p (GPa)	114.0 [37]	94.3 [37][54]	41.7[52][53]
G_p(GPa)	44.5 [37]	37.1 [37][54]	16.2[54]
E_s(HT) (GPa)	13.257	11.736	8.948
E_s(PB) (GPa)	15.705	14.310	10.194

Table 4-4 The calculation results of E changed by BMD from PB models

BMD(x) (g/cm^3)	E(Normal) (GPa)	E(OA) (GPa)	E(OP) (GPa)
>0.8	15.705 (2.625x-1.625)	14.310 (2.625x-1.625)	10.194 (2.625x-1.625)
0.8	7.98	7.27	5.18
0.75	7.13	6.49	4.63
0.7	6.37	5.80	4.13
0.65	5.68	5.17	3.69
0.6	5.05	4.60	3.28
0.55	4.47	4.07	2.90
0.5	3.93	3.58	2.55
0.45	3.42	3.12	2.22
0.4	2.94	2.68	1.91
0.35	2.50	2.27	1.62
0.3	2.07	1.89	1.35
0.25	1.67	1.52	1.09
0.2	1.29	1.18	0.84

Table 4-5 The calculation results of E changed by BMD from HT models

BMD(x) (g/cm^3)	E(Normal) (GPa)	E(OA) (GPa)	E(OP) (GPa)
>0.8	13.257 (2.625x-1.625)	11.736 (2.625x-1.625)	8.948 (2.625x-1.625)
0.8	6.74	5.96	4.55
0.75	6.02	5.33	4.06
0.7	5.37	4.76	3.63
0.65	4.79	4.24	3.24
0.6	4.26	3.77	2.88
0.55	3.77	3.34	2.55
0.5	3.31	2.93	2.24
0.45	2.89	2.56	1.95
0.4	2.48	2.20	1.68
0.35	2.11	1.86	1.42
0.3	1.75	1.55	1.18
0.25	1.41	1.25	0.95
0.2	1.09	0.97	0.74

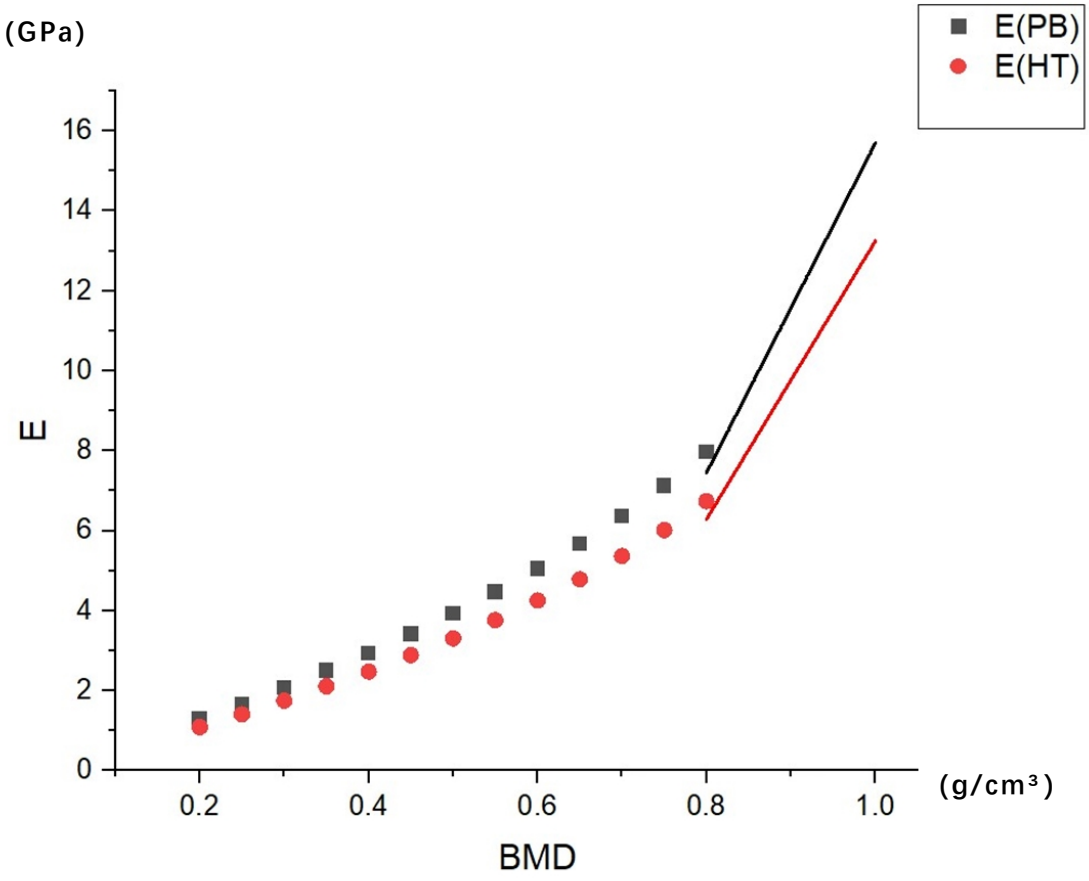

Fig.4-3 Variation of Young's modulus (E) with BMD for normal bones

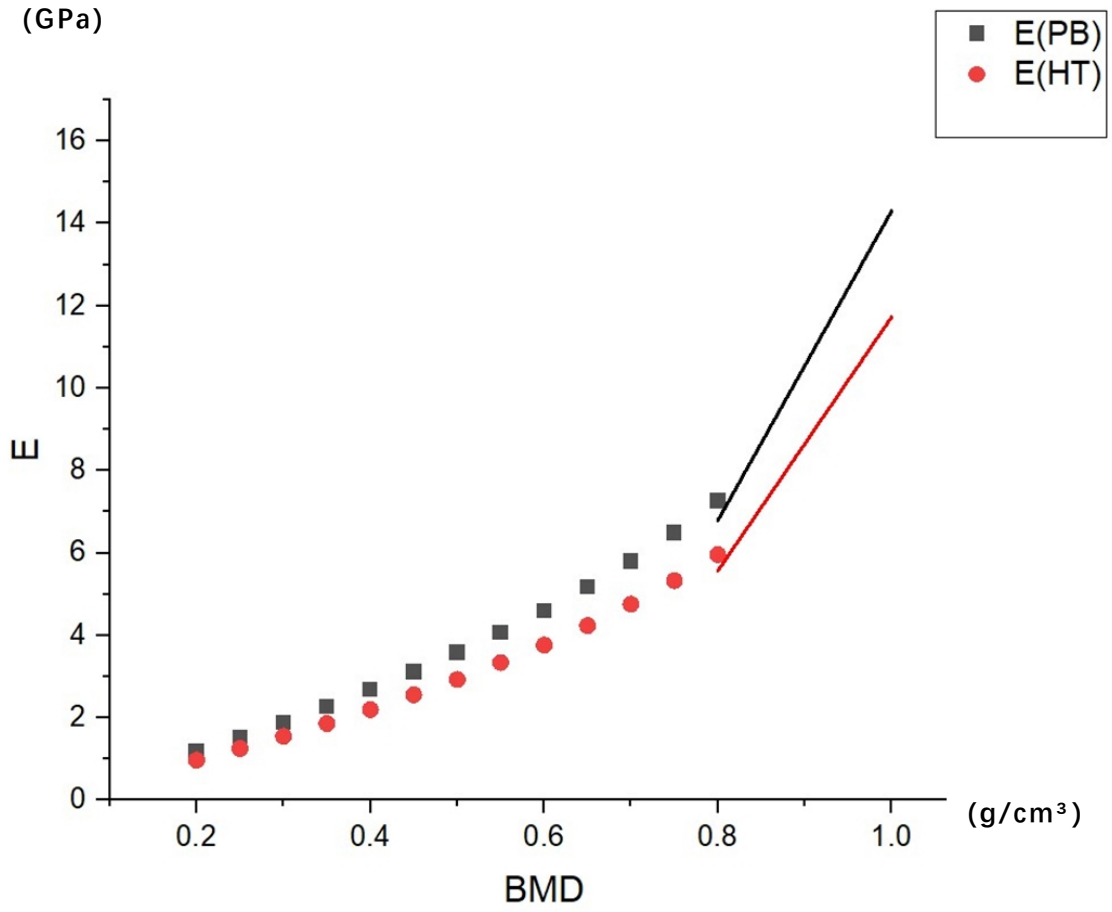

Fig.4-4 Variation of Young's modulus (E) with BMD for bones with osteopenia

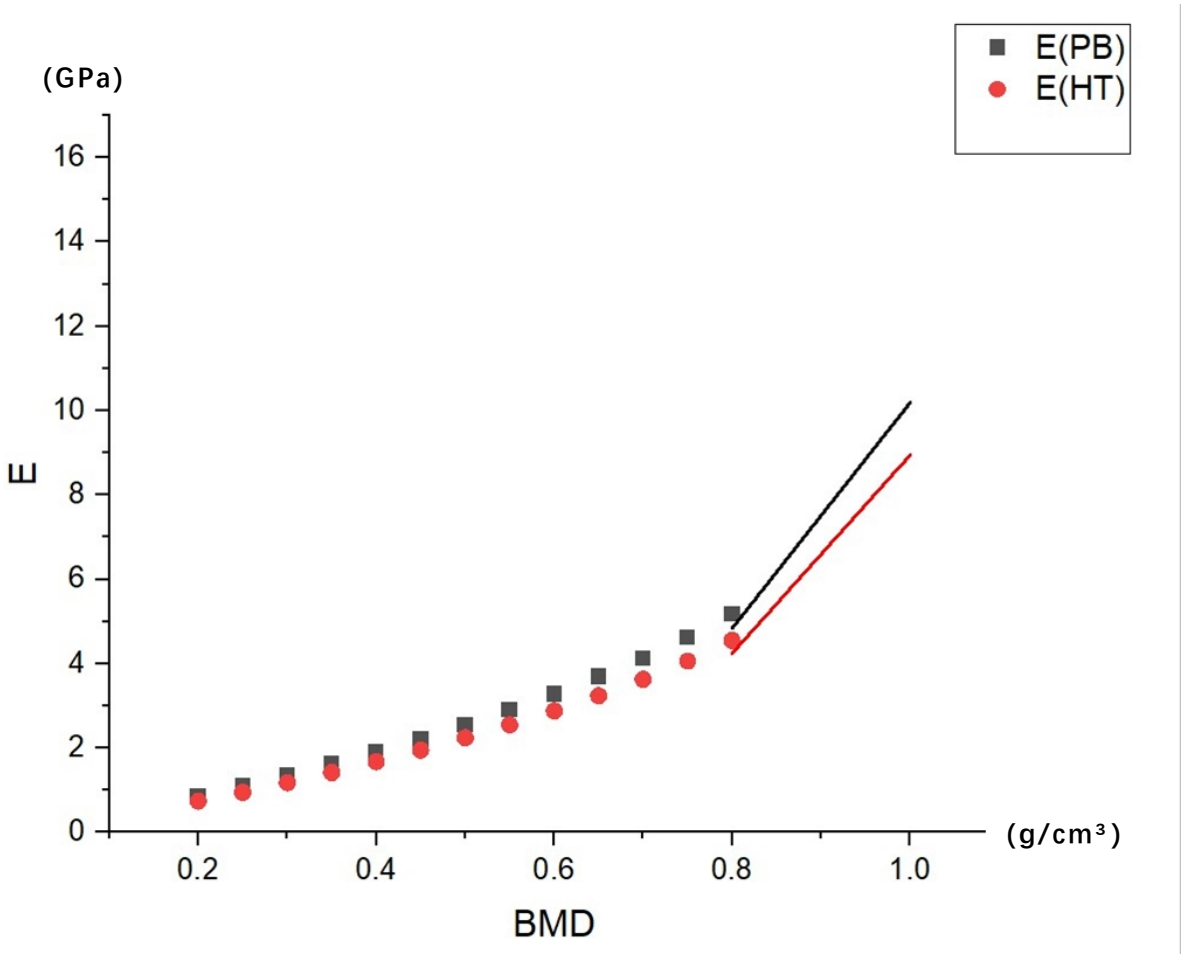

Fig.4-5 Variation of Young's modulus (E) with BMD for bones with osteoporosis

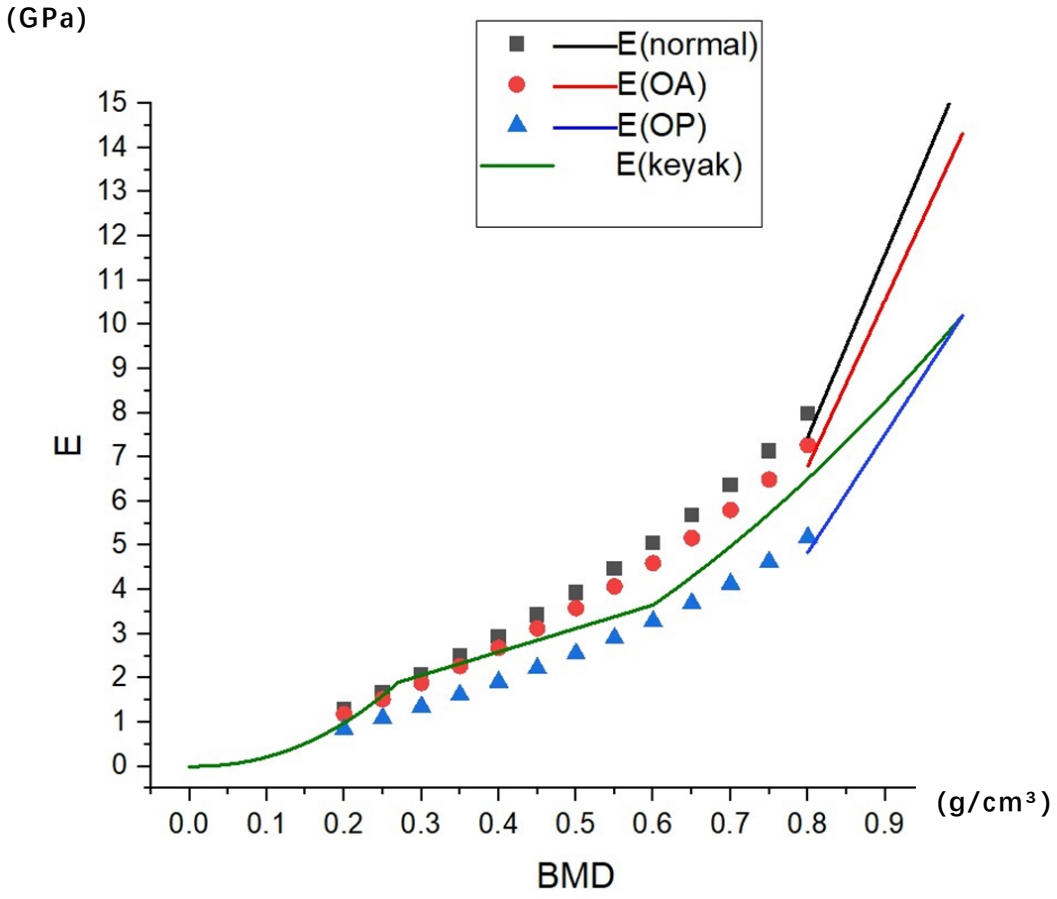

Fig.4-6 Variation of Young's modulus (E) with BMD from PB model

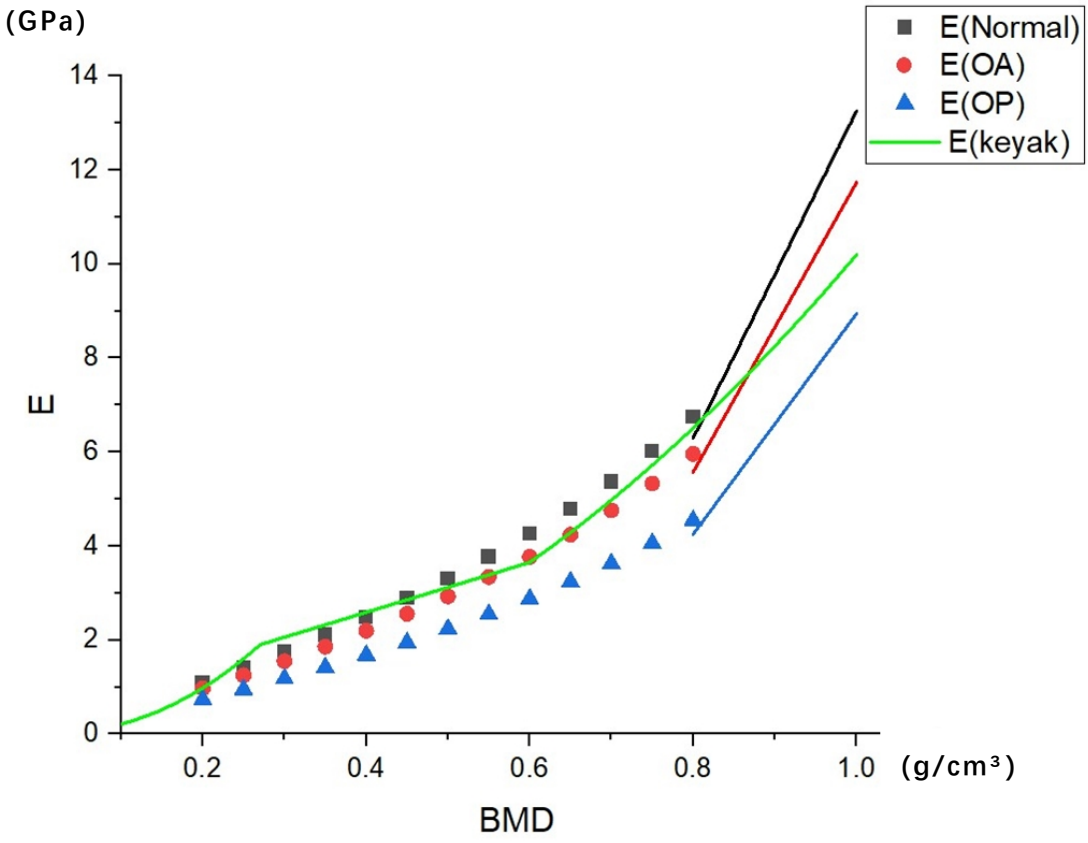

Fig.4-7 Variation of Young's modulus (E) with BMD from HT model

According to Fig.4-3,4-4 and 4-5, for normal bones, bones with osteopenia and bones with osteoporosis, the variation trend of E with BMD is similar to Keyak's model, and the results calculated by the PB model are generally higher than those calculated by the HT model.

Comparing the Fig.4-6 and 4-7, under the same conditions, the results obtained by using the HT model in the research are closer to Keyak's experimental results than the PB model. It proves that the HT model is more advantageous than the PB model in this stage of research.

4.4 Summary

In this phase, firstly, the concepts and diagnostic guidelines of osteopenia and osteoporosis are introduced. Then, we estimated separately using microscopic models for the variation of Young's modulus (E) with BMD for normal bones, bones with osteopenia and bons with osteoporosis. In this calculation process, the value of E_s was estimated by using the HT model and the PB model respectively. The calculations proves that for normal bones, bones with osteopenia and bones with osteoporosis, under the same conditions, the results obtained by using the HT model in the research are closer to Keyak's experimental results than the PB model. It proves that the HT model is more advantageous than the PB model in this stage of research.

5 Conclusion

In this study, the aim is to develop a theoretical model of the relationship between E and BMD. After introducing the basic knowledge of bone and the previous research by Keyak and Keller in phase 1, in phase 2, a macroscopic model was established based on the previous studies known from reading the paper. By comparing the data calculated by the macroscopic model, we find that the change trend of the results calculated by the macroscopic model is basically consistent with Keyak's model, but the overall value is higher than Keyak's results.

In phase 3,we considered the microstructure of bones, and revised the macroscopic model into microscopic model by adding consideration of the impact of loading angle on the value of E_s. In order to specifically calculate the impact of loading angle on E_s, for the two important paraments in the functions - E_1 and E_2, when determining their values, we used three different theoretical models - HT model, PB model and LWX model. Comparing the results of the calculation of Es in three models with the previous studies reviewed, we find the data calculated by HT and PB models match the data from the previous research, so only the HT and PB models will will continue to be used in research.

In phase 4, firstly, we introduced the concepts and diagnostic guidelines of osteopenia and osteoporosis. Then, we the variation of Young’s modulus (E) with BMD for normal bones, bones with osteopenia and bons with osteoporosis was

separately estimated by using the microscopic models. In this calculation process, the value of Es was estimated by using the HT model and the PB model respectively. The calculations proves that for normal bones, bones with osteopenia and bones with osteoporosis, under the same conditions, the results obtained by using the HT model in the research are closer to Keyak's experimental results than the PB model. It proves that the HT model is more advantageous than the PB model in this stage of research.

In this phase of research, we only performed theoretical calculations and no experimental modeling. CT-FEM is a research method that can better combine the theory in this study. FEM virtually divides an object with a complex structure into finite-sized elements. It is a method to approximate a structure by connecting adjacent elements at a node. It is a structural analysis method that derives the characteristics of the entire structure by substituting the boundary conditions of the amount of displacement for each element and predicts its strength and mechanical characteristics. Even if the object to be analyzed has a complex shape or a large structure, any shape can be expressed by selecting the appropriate shape and size of the elements. In addition, since the material properties are defined for each element, the material can be changed for each element. For example, it is possible to analyze the stress applied to the bone when an implant is inserted. CT-FEM is a method of applying FEM to images obtained by X-ray CT. A three-dimensional bone model is

created from X-ray CT images, and load conditions such as loads are given to it to predict deformation and destruction of the bone structure.[55]It shows the microscopic model can use to calculate and predict the properties of the finite-sized elements well, and compared with the experimental results of CT-FEM, so it seems that the application of the theory of this research in CT-FEM can be positively expected.

References

[1] Lee, Cassandra (January 2001). The Bone Organ System: Form and Function. Science Direct. Academic Press. pp. 3–20.

[2] e Buffrénil, Vivian; de Ricqlès, Armand J; Zylberberg, Louise; Padian, Kevin; Laurin, Michel; Quilhac, Alexandra (2021). Vertebrate skeletal histology and paleohistology (Firstiton ed.). Boca Raton, FL: CRC Press. pp. xii + 825.

[3] Hall, John (2011). Textbook of Medical Physiology (12th ed.). Philadelphia: Elsevier. pp. 957–960.

[4] Meyers, Marc André; Chen, Po-Yu; Lin, Albert Yu-Min; Seki, Yasuaki (1 January 2008). "Biological materials: Structure and mechanical properties". Progress in Materials Science. 53 (1): 1–206.

[5] Hall, Susan J. (2007). Basic Biomechanics with OLC (5th ed., Revised. ed.). Burr Ridge: McGraw-Hill Higher Education. p. 88.

[6]https://www.researchgate.net/figure/Illustration-of-the-bone-structure-at-a-macroscale-and-the-osteogenic-commitment-of_fig2_343698607

[7]https://www.sciencephoto.com/media/1183319/view/cortical-bone-light-micrograph

[8] https://en.wikipedia.org/wiki/Bone#/media/File:Spongy_bone_-_trabecules.jpg

[9] Jastrzebski, D. (1959). Nature and Properties of Engineering Materials (Wiley International ed.). John Wiley & Sons, Inc.

[10]https://en.wikipedia.org/wiki/Young%27s_modulus#/media/File:Stress_strain_ductile.svg

[11] Keyak, J. H., Lee, I. Y., & Skinner, H. B. (1994). Correlations between orthogonal mechanical properties and density of trabecular bone: use of different densitometric measures. Journal of biomedical materials research, 28(11), 1329-1336.

[12] Keyak, J. H., Rossi, S. A., Jones, K. A., & Skinner, H. B. (1997). Prediction of femoral fracture load using automated finite element modeling. Journal of biomechanics, 31(2), 125-133.

[13] Keller, T. S. (1994). Predicting the compressive mechanical behavior of bone. Journal of biomechanics, 27(9), 1159-1168.

[14] Currey, J. D. (1984) The Mechanical Adaptations of Bones. Princeton University Press, Princeton.

[15] Mohammadizadeh, SeyedMehdi; Moghaddam, Mehdi Azhdary; Talebbeydokhti, Naser (2021). "Analysis of Flow in Porous Media using Combined Pressurized-Free surface Network". Journal of Porous Media. Begel House Inc. 24 (10): 1–15.

[16] Su, Bao-Lian; Sanchez, Clément; Yang, Xiao-Yu, eds. (2011). Hierarchically Structured Porous Materials: From Nanoscience to Catalysis, Separation, Optics, Energy, and Life Science - Wiley Online Library.

[17] Cowin, S. C. (1999). Bone poroelasticity. Journal of biomechanics, 32(3), 217-238.

[18] Zhang, D., Weinbaum, S., & Cowin, S. C. (1998). Estimates of the peak pressures in bone pore water. Journal of Biomechanical Engineering, 120, 897-703

[19]https://stock.adobe.com/es/images/bone-structure-bone-tissue-close-up-osteoporosis/341477158?as_campaign=ftmigration2&as_channel=dpcft&as_campclass=brand&as_source=ft_web&as_camptype=acquisition&as_audience=users&as_content=closure_asset-detail-page

[20] Gibson, L. J. (1985). The mechanical behaviour of cancellous bone. Journal of biomechanics, 18(5), 317-328.

[21] Topoliński, T., Cichański, A., Mazurkiewicz, A., & Nowicki, K. (2012). The relationship between trabecular bone structure modeling methods and the elastic modulus as calculated by FEM. The Scientific World Journal, 2012.

[22] Keyak, J. H., Lee, I. Y., & Skinner, H. B. (1994). Correlations between orthogonal mechanical properties and density of trabecular bone: use of different densitometric measures. Journal of biomedical materials research, 28(11), 1329-1336.

[23] Wagner, H. D., & Weiner, S. (1992). On the relationship between the microstructure of bone and its mechanical stiffness. Journal of Biomechanics, 25(11), 1311-1320.

[24] Weiner, S., Arad, T., & Traub, W. (1991). Crystal organization in rat bone lamellae. FEBS letters, 285(1), 49-54.

[25] Cox, H. L. (1952) The elasticity and strength of paper and other fibrous materials.

Br. J. appl. Phys. 3, 72-79.

[26] Currey, J. D. (1962) Strength of bone. Nature 195, 513-514.

[27] Currey, J. D. (1969) The relationship between the stiffness and the mineral content of bone. J. Biomechanics 2, 477-480.

[28] Lang, S. B. (1969) Elastic coefficients of animal bone. Science,165,287-288.

[29] Reilly, D. and Burstein, A. H. (1975) The elastic and ultimate properties of compact bone tissue. J. Biomechanics 8, 393-405.

[30] Bonfield, W. and Grynpas, M. D. (1977) Anisotropy of the Young's modulus of bone. Nature 270, 453-454.

[31] Affdl, J. H., & Kardos, J. L. (1976). The Halpin-Tsai equations: a review. Polymer Engineering & Science, 16(5), 344-352.

[32] Weiner, S. and Traub, W. (1991) Organization of crystals in bone. In Mechanisms and Phylogeny of Mineralization in Biological Systems (Edited by Suga, S. and Nakahara, H.), pp. 247-253. Springer, Tokyo.

[33] Ashton, J. E., Halpin, J. C. and Petit, P. H. (1969) Primer on Composite Muteriak: Amzlysis. Technomic Publishing, Westport, CT.

[34] Padawer, G. E. and Beecher, N. (1970) On the strength and stiffness of planar reinforced plastic resins. Polym. Engng Sci. 10, 1851192.

[35]Lusis, J., Woodhams, R. T. and Xhantos, M. (1973) The effect of flake aspect ratio on the flexural properties of mica reinforced plastics. Polym. Engng Sci. 13, 139-145.

[36] Jackson, A. P., Vincent, J. F. V. and Turner, R. M. (1988) The mechanical design of nacre. Proc. R. Sot. Land. B234, 415-440.

[37] Gilmore, R. S. and Katz, J. L. (1982) Elastic properties of apatites. J. Mater. Sci. 17, 1131-1141.

[38] Tanioka, A., Tazawa, T., Miyasaka, K. and Ishikawa, K. (1974) Effects of water on the mechanical properties of gelatin films. Biopolymers 13, 735-746.

[39] Doty, S., Robinson, R. A. and Schofield, B. (1976) Morphology of bone and histochemical staining characteristics of bone cells. In Handbook of Physiology (Edited by Aurbach G. D.), pp. 3-23. American Physiology Sot., Washington, DC

[40] Hofmann, T., Heyroth, F., Meinhard, H., Fränzel, W., & Raum, K. (2006). Assessment of composition and anisotropic elastic properties of secondary osteon lamellae. Journal of biomechanics, 39(12), 2282-2294.

[41] Bonfield, W., & Grynpas, M. D. (1977). Anisotropy of the Young's modulus of bone. Nature, 270, 453-454.

[42] "Handout on Health: Osteoporosis". NIAMS. August 2014. Archived from the original on 18 May 2015. Retrieved 16 May 2015.

[43] Kim DH, Vaccaro AR (2006). "Osteoporotic compression fractures of the spine; current options and considerations for treatment". The Spine Journal. 6 (5): 479–487.

[44] Cranney A, Jamal SA, Tsang JF, Josse RG, Leslie WD (September 2007). "Low bone mineral density and fracture burden in postmenopausal women". CMAJ. 177 (6):

575–80

[45] Wright NC, Looker AC, Saag KG, Curtis JR, Delzell ES, Randall S, Dawson-Hughes B (November 2014). "The recent prevalence of osteoporosis and low bone mass in the United States based on bone mineral density at the femoral neck or lumbar spine". Journal of Bone and Mineral Research. 29 (11): 2520–6.

[46] https://www.sohu.com/a/314397490_100012999

[47] "Bone mineral density test". U.S. National Library of Medicine.

[48] WHO Scientific Group on the Prevention and Management of Osteoporosis (2000 : Geneva, Switzerland) (2003). Prevention and management of osteoporosis : report of a WHO scientific group, pp. 7, 31.

[49] WHO (1994). "Assessment of fracture risk and its application to screening for postmenopausal osteoporosis. Report of a WHO Study Group". World Health Organization Technical Report Series. 843: 1–129.

[50] 原発性骨粗鬆症の診断基準(2012 年度改訂版)；日本骨代謝学会.

[51]https://wenku.baidu.com/view/d4cc327180c758f5f61fb7360b4c2e3f572725e5.html

[52] Gilmore, R. S., Pollack, R. P., & Katz, J. L. (1970). Elastic properties of bovine dentine and enamel. Archives of oral Biology, 15(8), 787-IN17.

[53] Nikodem, A. (2012). Correlations between structural and mechanical properties of human trabecular femur bone. Acta of Bioengineering & Biomechanics, 14(2).

[54] Arkusz, K., Klekiel, T., Niezgoda, T. M., & Będziński, R. (2018). The influence

of osteoporotic bone structures of the pelvic-hip complex on stress distribution under impact load. Acta of Bioengineering and Biomechanics, 20(1), 29-38.

[55] 大久保知幸，森浩一，和田野安良，川波公香，橘香織，清水如代，& 関根紀夫. (2013). X 線 CT 画像を用いた有限要素解析による腰椎圧迫骨折のリスク予測. 日本保健科学学会誌, 16(2), 90-98.

Acknowledgements

I offer my enduring gratitude to my advisor Prof. Mitsugu Todo, who has welcomed me beyond my expectations and gave me the opportunity to study in Japan. He also gave me many guidance to help me finish my master research.

I especially thank my senior Mr. Meng Xiang Xiang, who has greatly given me both academical and living support. He spent a lot of his personal time helping me to quickly integrate into the life of studying in Japan.

I thank Mr. Takeuchi Ryo, Mr. Shiiya Sena, Mr. Naito Daisuke, Mr. Shirazawa Ren. I learned a lot in the seminars with them.

Above all, I am forever indebted to my family, for their love, their support, for everything they give me and everything I have in my life.